

THE ANALYSIS OF LIQUID LOADING PROBLEMS  
IN HYDRAULICALLY FRACTURED GAS WELLS

A Thesis

by

CHARLES EDWARD PIETSCH

(Fuzzy)

Submitted to the Graduate College of  
Texas A & M University  
in partial fulfillment of the requirements for the degree of  
MASTER OF SCIENCE

August 1986

Major Subject: Petroleum Engineering

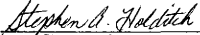
THE ANALYSIS OF LIQUID LOADING PROBLEMS  
IN HYDRAULICALLY FRACTURED GAS WELLS

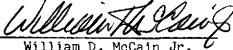
A Thesis

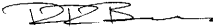
by

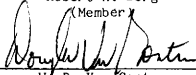
CHARLES EDWARD PIETSCH

Approved as to style and content by:

  
\_\_\_\_\_  
Stephen A. Holditch  
(Chairman of Committee)

  
\_\_\_\_\_  
William D. McCain Jr.  
(Member)

  
\_\_\_\_\_  
Robert R. Berg  
(Member)

  
\_\_\_\_\_  
W. D. Von Gonten  
(Head of Department)

August 1986

## ABSTRACT

The Analysis of Liquid Loading Problems  
in Hydraulically Fractured Gas Wells (August 1986)  
Charles Edward Pietsch, B.S., Texas A&M University  
Chairman of Advisory Committee: Dr. S. A. Holditch

Liquid loading problems in hydraulically fractured gas wells have been investigated using a two-phase, two-dimensional computer model. A data base from an analysis of twenty wells completed in the Cotton Valley Lime was used to study the effect that certain parameters have on long term production. The parameters which were investigated were the effects of gas and water relative permeability, gas permeability hysteresis, capillary pressure, and formation damage. Also, the history-match of production data was made to verify that the model can actually simulate the liquid loading that occurs in these twenty wells.

It has been determined that the fracture fills up with liquids because the liquid is not efficiently removed from the wellbore. This indicates that the fracture is merely an extension of the wellbore. The presence of a saturated region around the fracture caused by the imbibition of fracture fluid has very little effect on long term production if the liquid in the wellbore is continuously removed. Finally, the cleanup period following a hydraulic fracture treatment can last several weeks before gas production begins. This occurs when the irreducible gas saturation is greater than 30 percent and the fracture fluid remains immobile around the fracture.

## ACKNOWLEDGEMENTS

The author would like to express his sincere appreciation to the following individuals for their contribution in this thesis:

Dr. Stephen A. Holditch for his guidance and support during the course of this work which were more valuable than words can describe;

Mitchell Energy Corp. and the Crisman Institute for the field data from twenty gas wells completed in the Cotton Valley Lime, without which, this thesis would not have been possible;

Dr. W. D. McCain and Dr. R. R. Berg for serving as members of the author's advisory committee.

TABLE OF CONTENTS

	Page
ABSTRACT . . . . .	iii
ACKNOWLEDGEMENTS . . . . .	iv
TABLE OF CONTENTS . . . . .	v
LIST OF TABLES . . . . .	vii
LIST OF FIGURES . . . . .	ix
INTRODUCTION . . . . .	1
DETERMINATION OF RESERVOIR PROPERTIES . . . . .	6
Description of Cotton Valley Lime Wells . . . . .	6
Method of Analysis . . . . .	6
CLASSIFICATION OF WELLS . . . . .	24
ANALYSIS OF LIQUID LOADING . . . . .	29
Relative Permeability Functions . . . . .	29
Capillary Pressure Functions . . . . .	32
The Fracture . . . . .	32
The Saturated Region . . . . .	36
Production Runs and Injection Runs . . . . .	36
Effects of Various Parameters on Long Term Production . . . . .	39
Effect of Relative Permeability to Water . . . . .	39
Effect of Relative Permeability to Gas . . . . .	42
Effect of Gas Permeability Hysteresis . . . . .	44
Effect of Capillary Pressure . . . . .	61
Effect of Formation Damage . . . . .	63
Calibrating the Reservoir Model for Liquid Loading . . . . .	66
Effect of Liquid Buildup In and Around the Fracture . . . . .	70
CONCLUSIONS . . . . .	82
NOMENCLATURE . . . . .	86
REFERENCES . . . . .	87
APPENDIX A COMPUTER MODEL PROPTRAN . . . . .	89
APPENDIX B COMPUTER MODEL TYPEFIN . . . . .	93

## TABLE OF CONTENTS (continued)

	Page
APPENDIX C COMPUTER MODEL FRACSIM . . . . .	96
APPENDIX D COMPUTER MODEL GASWAT . . . . .	102
VITA . . . . .	107

## LIST OF TABLES

TABLE	Page
1 Results of Log Analysis by Mitchell Energy Corp. . . . .	8
2 Values for Formation Permeability from Pre-Fracture Buildup Test Analysis . . . . .	9
3 Results of Determination of Gross and Net Fracture Height for Computer Model PROPTRAN . . . . .	12
4 Initial Estimates of Fracture Half Length and Formation Permeability using Computer Models PROPTRAN and TYPEFIN . . . . .	15
5 Comparison of History-Matched Parameters With the Computer Model TYPEFIN when using Two Different Sets of Fracture Fluid Data . . . . .	19
6 Refinement of History-Matched Parameters using the Computer Model FRACSIM . . . . .	22
7 Production Values for the Cotton Valley Lime Wells . . . . .	26
8 Average Reservoir Properties Characterizing the Cotton Valley Lime . . . . .	28
A-1 Input Data for Computer Model PROPTRAN . . . . .	90
A-2 Fracture Dimension Analysis using Computer Model PROPTRAN . . . . .	91
A-3 Proppant Transport Analysis using Computer Model PROPTRAN . . . . .	92
B-1 Input Data for Computer Model TYPEFIN . . . . .	94
B-2 Well Performance Predicted by Computer Model TYPEFIN . . . . .	95
C-1 Grid Patterns used for Computer Model FRACSIM . . . . .	97
C-2 Input Data for Computer Model FRACSIM . . . . .	98
C-3 Fracture Closure for 20/40 Mesh Sand . . . . .	99
C-4 Time Step from Computer Model FRACSIM . . . . .	100
C-5 Summary Table from Computer Model FRACSIM . . . . .	101
D-1 Grid Patterns used for Computer Model GASWAT . . . . .	103

## LIST OF TABLES (continued)

TABLE	Page
D-2 Input Data for Computer Model GASWAT . . . . .	104
D-3 Time Step from Computer Model GASWAT . . . . .	105
D-4 Summary Table from Computer Model GASWAT . . . . .	106



## LIST OF FIGURES

FIGURE	Page
1 Openhole Log for the Engram No. 1 Well . . . . .	10
2 Proppant Concentration for the Engram No. 1 Well . . . . .	13
3 Proppant Concentration for the Engram No. 1 Well using Adjusted Values of $n'$ and $K'$ . . . . .	17
4 History-Match of Production Data for the Prichard No. 1 Well using the Computer Model TYPEFIN for $K=0.001$ md and $XF=900$ ft . . . . .	20
5 History-Match of Production Data for the Prichard No. 1 Well using the Computer Model FRACSIM for $K=0.0012$ md and $XF=900$ ft . . . . .	23
6 Classification of Cotton Valley Lime Wells using Formation Permeability . . . . .	25
7 Gas Relative Permeability Curves used in Analysis of Liquid Loading . . . . .	30
8 Water Relative Permeability Curves used in Analysis of Liquid Loading . . . . .	31
9 Capillary Pressure Curve for an Edwards Limestone Core Sample with a Porosity of 5.9% and a Permeability of 0.12 md . . . . .	33
10 Capillary Pressure Curve for a Tight Gas Sandstone Core Sample with a Porosity of 10% and a Permeability of 0.0017 md . . . . .	34
11 Capillary Pressure Curve Which Represents an Average Tight Gas Core Sample with a Porosity of 8% and a Permeability of 0.01 md . . . . .	35
12 Areal View of Drainage Area . . . . .	37
13 Grid Pattern used to Model 1/4 of the Drainage Area using the Computer Model GASWAT . . . . .	38
14 Effect of Relative Permeability to Water on Long Term Production using the Average Cotton Valley Lime Data Set for KRG1 and PCGW1 Curves . . . . .	40

## LIST OF FIGURES (continued)

FIGURE	Page
15 Effect of Relative Permeability to Water on Water Production using the Average Cotton Valley Lime Data Set for KRG1 and PCGW1 Curves . . . . .	41
16 Effect of Saturated Region on Water Production using the Average Cotton Valley Lime Data Set for KRG1 and PCGW1 Curves . . . . .	43
17 Normalized Relative Permeability to Gas Curves used in the Analysis of Liquid Loading . . . . .	45
18 Effect of Relative Permeability to Gas on Long Term Production using the Average Cotton Valley Lime Data Set for KRW1 and PCGW1 Curves . . . . .	46
19 Effect of the Parameter LAMDA on Gas Permeability Hysteresis when using the Killough Method . . . . .	48
20 Effect of Hysteresis on Relative Permeability to Gas when using a LAMDA of 1 . . . . .	49
21 Effect of Gas Permeability Hysteresis on Short Term Production using the Average Cotton Valley Lime Data Set for LAMDA of 1 and KRG1, KRW3, and PCGW1 Curves . . . . .	51
22 Effect of Gas Permeability Hysteresis on Long Term Production using the Average Cotton Valley Lime Data Set for LAMDA of 1 and KRG1, KRW3, and PCGW1 Curves . . . . .	52
23 Effect of Gas Permeability Hysteresis on Short Term Production using the Average Cotton Valley Lime Data Set for LAMDA of 1 and KRG1, KRW1, and PCGW1 Curves . . . . .	53
24 Effect of Gas Permeability Hysteresis on Long Term Production using the Average Cotton Valley Lime Data Set for LAMDA of 1 and KRG1, KRW1, and PCGW1 Curves . . . . .	54
25 Effect of Hysteresis on Relative Permeability to Gas when using a LAMDA of 2 . . . . .	56
26 Effect of Gas Permeability Hysteresis on Long Term Production using the Average Cotton Valley Lime Data Set for LAMDA of 2 and KRG1, KRW3, and PCGW1 Curves . . . . .	57

## LIST OF FIGURES (continued)

FIGURE	Page
27 Effect of Gas Permeability Hysteresis on Short Term Production using the Average Cotton Valley Lime Data Set for LAMDA of 2 and KRG1, KRW3, and PCGW1 Curves . . . . .	58
28 Effect of Gas Permeability Hysteresis on Long Term Production using the Average Cotton Valley Lime Data Set for LAMDA of 2 and KRG1, KRW1, and PCGW1 Curves . . . . .	59
29 Effect of Gas Permeability Hysteresis on Short Term Production using the Average Cotton Valley Lime Data Set for LAMDA of 2 and KRG1, KRW1, and PCGW1 Curves . . . . .	60
30 Effect of Capillary Pressure on Long Term Production using the Average Cotton Valley Lime Data Set for KRG1 and KRW1 Curves . . . . .	62
31 Effect of Displacement Pressure on Long Term Production using the Average Cotton Valley Lime Data Set for KRG1 and KRW1 Curves . . . . .	64
32 Effect of Formation Damage on Long Term Production using the Average Cotton Valley Lime Data Set for KRG1, KRW3, and PCGW1 Curves . . . . .	65
33 History-Match of Production Data for the Prichard No. 1 Well using the Computer Model GASWAT for $K=0.0017$ md and $XF=900$ ft . . . . .	67
34 History-Match of Production Data for the Prichard No. 1 Well using Different Values of $Q_{MIN}$ and the Computer Model GASWAT for $k=0.0017$ md and $XF=900$ ft . . . . .	69
35 History-Match of Water Production for the Prichard No. 1 Well using the Computer Model GASWAT for $k=0.0017$ md and $XF=900$ ft . . . . .	71
36 Effect of $Q_{MIN}$ on Long Term Production using the Below Average Cotton Valley Lime Data Set for KRG3, KRW3, and PCGW1 Curves . . . . .	73
37 Effect of Relative Permeability to Water using the Below Average Cotton Valley Lime Data Set and $Q_{MIN}$ for KRG3 and PCGW1 Curves . . . . .	76

## LIST OF FIGURES (continued)

FIGURE	Page
38 Effect of Formation Damage on Long Term Production using the Below Average Cotton Valley Lime Data Set & QMIN for KRG1, KRW1 and PCGW1 Curves . . . . .	77
39 Effect of Capillary Pressure on Long Term Production using the Below Average Cotton Valley Lime Data Set and QMIN for KRG3, KRW3, and PCGW1 Curves . . . . .	79
40 Effect of Reducing Capillary Pressure on Long Term Production using the Below Average Cotton Valley Lime Data Set and QMIN for KRG3, KRW3, and PCGW1 Curves . . . . .	80

## INTRODUCTION

The presence of liquids in and around the wellbore of a gas well can lead to liquid loading problems. A gas well begins to load up with liquids when there is insufficient energy to continuously lift the liquid from the wellbore. This happens when the velocity of the liquid decreases to a value that is less than the velocity of the gas in the wellbore. At this point, the liquid begins to produce in slugs, and unless the well has enough pressure to lift the slugs of liquid out of the wellbore, the liquid accumulates in the wellbore and severely reduces the gas production.

Several papers have been published concerning the calculation of a minimum or critical gas velocity.<sup>1-4</sup> The minimum gas velocity is used as a criterion to predict when a gas well will begin to load up with liquid. Duggan<sup>1</sup> was the first to present an empirical method for estimating the flow rate required to keep a gas well unloaded. However, it was developed for a specific type of gas reservoir. Therefore, it cannot be used as a general method for estimating the critical gas velocity. In 1969 Turner, et al.,<sup>2</sup> presented a more general method for determining the critical gas velocity. It considers the entrainment of liquid drops in the gas stream as the controlling factor in removing the liquid from the wellbore. Despite the fact that the Turner, et al. method is more general for estimating the critical gas velocity,

comparisons with field data indicates the need for more accurate prediction models.<sup>3</sup>

To remove the liquid from the wellbore, the gas velocity in the wellbore has to be increased. The two most common ways of achieving a higher gas velocity are by decreasing the flowing tubing pressure or decreasing the cross-sectional area of the tubing. Other methods of lifting the liquid from the wellbore include the use of pumping units, soap or foam injection, a liquid divertor gas-lift system, and a plunger lift. Pumping units are mainly used in shallow, low pressure gas wells where the liquids produced exceed 10 BPD,<sup>5</sup> and they are now being used in deep gas wells with the aid of a fiberglass rod string.<sup>6</sup> For wells with a high water-condensate ratio, the use of soap or foam injection has worked best at removing the liquid from the wellbore,<sup>5,7</sup> while the liquid divertor gas-lift system performs best in deeper, high abandonment pressure fields.<sup>5</sup> Finally, the plunger lift works well for wells that are of moderate depth and have an average flow rate of 20-50 Mcf/D.<sup>5</sup> However, all of these methods deal only with the liquid loading in the wellbore and do not address the liquid loading problem in the reservoir.

It has been observed in practice that the liquid loading problem is not always solved by just increasing the gas velocity in the wellbore. It has been hypothesized that the liquid loading problem actually extends in to the reservoir around the fracture. The presence of a high liquid saturated zone around the fracture could be part of the problem

and must be removed prior to experiencing any significant improvement in well productivity.

For hydraulically fractured gas wells, both Tannich<sup>8</sup> and Holditch<sup>9</sup> studied the effect that fracture fluid has around the fracture. Tannich studied the effects that fracture length, fracture conductivity, and formation permeability have on the cleanup period of a fractured well. He combined four different models in order to investigate their effect. These models were: (1) a two-phase, one-dimensional tubing model, (2) a two-phase, one-dimensional model to calculate fluid flow in the fracture, (3) a two-phase model using Buckley-Leverett equations to describe the flow behavior in the invaded zone around the fracture, and (4) a two-dimensional, single-phase model for calculating gas flow in the reservoir. In developing his composite model, Tannich neglected the effects of gravity and capillary pressure, and assumed that there was no mobile water in the reservoir. He concluded that permanent productivity damage is not likely if the fracture conductivity is relatively high compared to the formation permeability. Also, he concluded that the cleanup period is shorter for wells with a smaller fracture length and/or a higher formation permeability.

Holditch studied the effects that reservoir damage, gas and water relative permeability, permeability hysteresis, and capillary pressure have on the cleanup period following fracturing. He used a single-phase, two-dimensional, finite difference model to study the effect of reservoir damage around the fracture, and a two-phase, two-dimensional, fully implicit finite difference model to investigate the effects that

relative permeability and capillary pressure have on the performance of a hydraulically fractured reservoir. Holditch concluded that if the pressure drawdown does not exceed the formation capillary pressure and the water mobility is so low that the fracture fluid remains essentially immobile next to the fracture, gas production can be severely curtailed. However, if the pressure drop is much greater than the capillary pressure in the formation, no serious water block to gas flow will occur.

Both Tannich and Holditch limited their studies to the cleanup period following a hydraulic fracture treatment. Also, they both used less than 2000 barrels of fluid around the fracture. This amount is less than 20 percent of the fluid which will be used in this study.

The purpose of this research was to investigate the liquid loading problem in the reservoir and around the fracture and to determine if indeed it is a problem and what could be done to the reservoir to minimize the liquid loading problem. This was accomplished by using a data base from an analysis of 20 wells completed in the Cotton Valley Lime in East Texas. The reservoir properties of these wells were estimated using openhole logs, pressure buildup tests, fracture treatment data, and production data. In addition, average data sets were determined from the twenty wells that characterized (1) an above average well, (2) a below average well, and (3) an average well completed in the Cotton Valley Lime. Using these average data sets, the effects of gas and water relative permeability, gas permeability hysteresis, capillary



pressure and formation damage on long term production were investigated to determine how to minimize the liquid loading problem.

For the reservoir properties simulated in this research, the presence of a high liquid saturated zone around the fracture that was caused by the imbibition of fracture fluid has very little effect on long term production when the liquid in the wellbore is continuously removed. Also, the cleanup period following a hydraulic fracture treatment can last several weeks before gas production begins. This occurs when the irreducible gas saturation is greater than 30 percent and the fracture fluid remains immobile around the fracture.

## DETERMINATION OF RESERVOIR PROPERTIES

### Description of Cotton Valley Lime Wells

The data base for this research comes from twenty wells completed in the Cotton Valley Lime. These wells are operated by Mitchell Energy Corp. and are located in Fallon and North Personville fields, in Limestone County, Texas.

The Cotton Valley Lime is of Jurrassic age and is located on the west flank of the East Texas basin. It ranges in thickness from 300-500 ft and is overlain by 800 ft of Bossier shale.

The Cotton Valley Lime has been developed for natural gas since its discovery in 1969. Due to its initial low flow rate and low formation permeability, each well must be hydraulically fractured. The hydraulic fracture treatments on the twenty wells included in this study varied from pumping 300-800 thousand gallons of fracture fluid and 250-2700 thousand pounds of 20/40 mesh sand. Since less than 40 percent of the fracture fluid is initially produced back, a zone of high water saturation is established around the fracture. The excess water around the fracture may decrease the flow of gas towards the wellbore and eventually cause the gas flow rate to decline rapidly. Therefore, these wells can be used to prove or disprove the hypothesis that the liquid loading extends into the reservoir around the fracture.

### Method of Analysis

Reservoir properties of the twenty wells were determined using the openhole logs, pressure buildup tests, fracture treatment data and

production data. The reservoir properties of the twenty Cotton Valley Lime wells were used to build average data sets to investigate the liquid loading problem in the reservoir around the fracture.

The openhole logs were used to determine the porosity, net pay and average water saturation for each of the twenty Cotton Valley Lime wells. These values were reported by Mitchell Energy Corp.<sup>10</sup> and are used in this study. Table 1 summarizes the results presented by Mitchell Energy Corp.

The initial estimates of formation permeability were determined from five pre-fracture pressure buildup tests. Both the Horner method<sup>11</sup> and a type-curve matching method<sup>12,13</sup> were used with the aid of a computer program called GASTEST to calculate formation permeability. The computer program GASTEST was used to change bottom-hole shut-in pressure to adjusted pseudopressure. The Horner method was used to analyze the buildup test when the middle-time region (MTR) appeared on a semi-log graph of shut-in pressure vs. time. However, the middle-time region appeared in only three of the five buildup tests. Therefore, type curves were also used in analyzing the buildup tests. The type-curve matching technique used type curves developed by both Gringarten<sup>12</sup> and Cinco.<sup>13</sup> The estimates of formation permeability using both the Horner method and the Gringarten and Cinco type curves compare very well, as illustrated in Table 2. The formation permeabilities ranged from 0.0017 to 0.035 md.

The propped fracture dimensions were estimated using the fracture treatment data and a computer model called PROPTRAN. The computer model

TABLE 1  
Results of Log Analysis by Mitchell Energy Corp.

Well	Porosity %	Net Pay ft	Water Saturation %
Engram No. 1	7.2	97.5	13.0
Getty Muse No. 1	6.7	38.5	25.2
Vance No. 1	5.0	28.5	15.6
McFerran No. 1	5.9	163.0	39.3
Hawkins No. 1	6.1	31.0	15.5
Muse Duke No. 1	8.5	41.0	17.1
Croft No. 1	6.1	55.0	12.2
Muse A No. 1	6.1	46.0	24.6
Webb No. 1	5.3	62.5	34.1
Muse Tucker No. 1	5.7	70.5	24.1
Presley Sadler No. 1	5.3	106.0	23.1
Prichard No. 1	5.7	49.0	12.7
Kerr No. 1	6.0	45.0	41.9
Fenton No. 1	5.0	37.0	12.5
Truett No. 1	5.9	73.0	20.5
Jackson B No. 1	7.0	91.5	11.2
Ferguson No. 2	8.4	68.5	11.1
Smythe No. 1	6.7	122.0	25.7
Renfro No. 1	6.3	54.0	6.0
Lawrence No. 1	7.2	50.0	23.0

PROPTRAN is a proppant transport model which calculates the propped fracture dimensions. More information about the model PROPTRAN and its purpose is given in Appendix A.

TABLE 2  
Values for Formation Permeability  
from Pre-Fracture Buildup Test Analysis

Well	Horner Method md	Gringarten Type Curve md	Cinco Type Curve md
Hawkins No. 1	No MTR	0.0146	0.0148
Getty Muse No. 1	0.0351	0.0349	0.0327
Lawrence No. 1	0.0130	0.0141	0.0130
Presley Sadler No. 1	0.0017	0.0017	0.0021
Vance No. 1	No MTR	0.0021	-

In order to determine the propped fracture dimensions, values of gross and net fracture height had to be determined. The openhole logs were used to compute these values. To assure consistency in the selection of gross fracture height, the top of the fracture was assumed to grow 20 ft into the Bossier shale, and the bottom of the fracture was estimated to extend 50 ft below the lowest perforation. The openhole log for the Engram No. 1 well is shown in Figure 1. The top of the Cotton Valley Lime is located at a depth of 10736 ft. The lowest perforation was shot at a depth of 11043 ft. Therefore, the top and bottom of the fracture was estimated to be 10716 and 11093 ft,

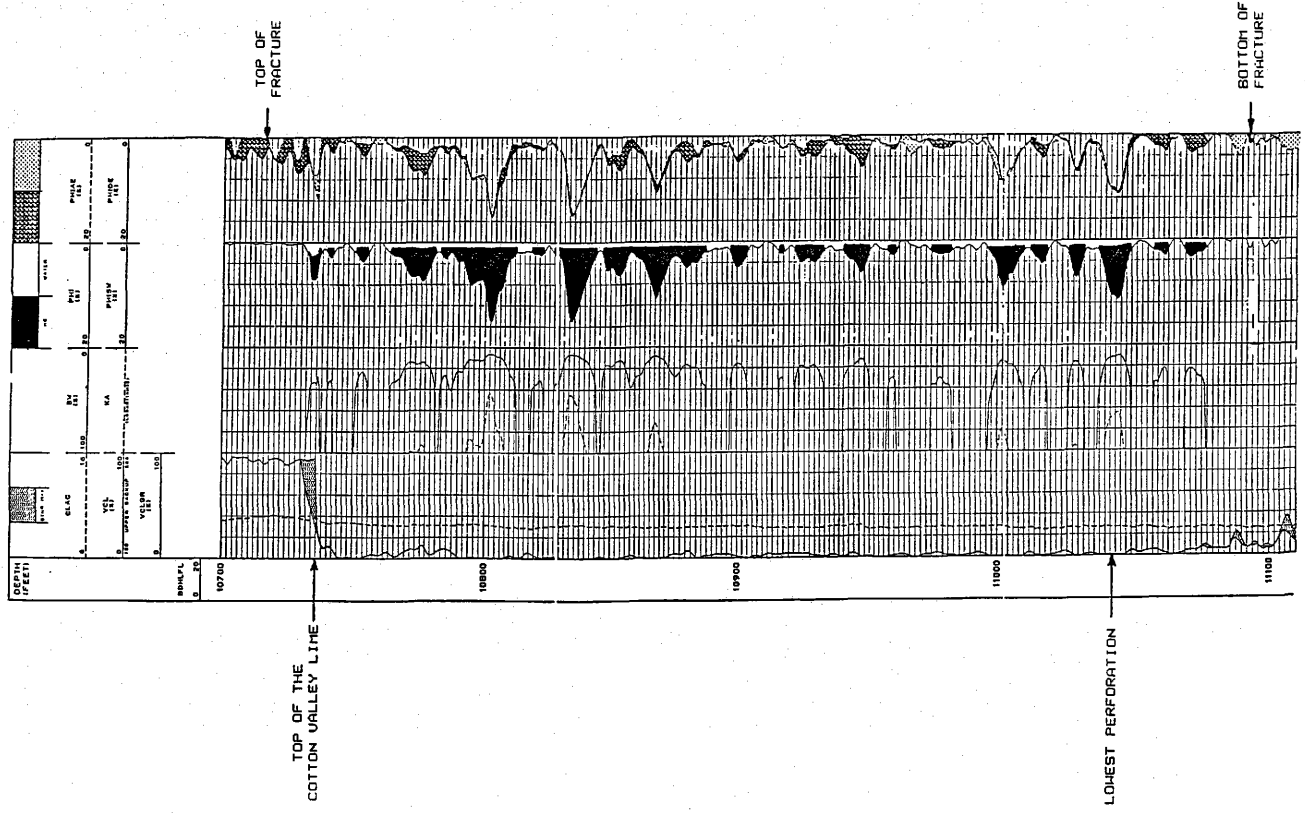


Fig. 1 - Openhole Log for the Engrum No. 1 Well

respectively. This resulted in a gross fracture height of 377 ft for the Engram No. 1 well.

The net fracture height, or amount of height that will take leakoff, was determined using a four percent porosity cutoff. This value was used because log-derived porosities above four percent matched the core data very well.<sup>10</sup> Also, it was questionable whether matrix porosities below four percent would take any fluid since regular core analysis indicated that zones with porosities below this value had essentially no measurable permeability. The net fracture height for the Engram No. 1 well was determined to be 114 ft. The same method of analysis was used to determine the gross and net fracture height for each well. These values are presented in Table 3.

Knowing the values of gross and net fracture height, the propped fracture length and fracture conductivity were determined using the computer model PROPTRAN. Figure 2 illustrates the proppant concentration down the fracture for the Engram No. 1 well. The shaded area represents the location of net pay within the fracture. The effective propped fracture length was determined using a proppant concentration of 0.5 lb/ft<sup>2</sup> and the location of net pay within the fracture. A proppant concentration of 0.5 lb/ft<sup>2</sup> was used as a cutoff because the fracture conductivity decreases rapidly below this value. The effective propped fracture length was determined as

$$\overline{XF} = \frac{\sum(XF * H)}{\sum H} \dots \dots \dots (1)$$

TABLE 3  
 Results of Determination of Gross and Net Fracture  
 Height for Computer Model PROPTRAN

Well	Gross Fracture Height ft	Net Fracture Height ft
Engram No. 1	377	114
Getty Muse No. 1	234	40
Vance No. 1	285	30
McFerran No. 1	313	177
Hawkins No. 1	276	25
Muse Duke No. 1	265	44
Croft No. 1	218	70
Muse A No. 1	336	67
Webb No. 1	261	69
Muse Tucker No. 1	278	72
Presley Sadler No. 1	403	129
Prichard No. 1	247	54
Kerr No. 1	220	60
Fenton No. 1	339	63
Jackson B No. 1	414	71
Ferguson No. 2	297	98
Smythe No. 1	232	73
Renfro No. 1	394	135
Lawrence No. 1	262	49



PROPPANT CONCENTRATIONS EXPRESSED IN LB/FT<sup>2</sup>

L E N G T H \* \* F T

	0.	393.	787.	1180.	1574.	1967.	2361.	2754.	3147.	3541.	3934.
H 379.	1.62	1.38	0.75	0.25	0.07	0.00	0.00	0.00	0.00	0.00	0.00
E 341.	1.62	1.49	1.38	0.85	0.42	0.03	0.00	0.00	0.00	0.00	0.00
I 303.	1.62	1.49	1.35	1.24	1.10	0.08	0.00	0.00	0.00	0.00	0.00
G 265.	1.62	1.49	1.35	1.25	1.31	0.10	0.00	0.00	0.00	0.00	0.00
H 227.	1.62	1.49	1.35	1.25	1.31	0.11	0.00	0.00	0.00	0.00	0.00
T 189.	1.62	1.49	1.35	1.25	1.31	0.11	0.00	0.00	0.00	0.00	0.00
152.	1.62	1.49	1.35	1.25	1.31	0.11	0.00	0.00	0.00	0.00	0.00
114.	1.62	1.49	1.35	1.25	1.31	0.11	0.00	0.00	0.00	0.00	0.00
76.	1.62	1.49	1.35	1.25	1.31	0.11	0.00	0.00	0.00	0.00	0.00
F 38.	1.62	1.49	1.35	1.25	1.31	0.11	0.00	0.00	0.00	0.00	0.00
T 0.	1.62	1.59	1.91	2.34	3.68	0.68	0.00	0.00	0.00	0.00	0.00

0.5 lb/ft<sup>2</sup>

Fig. 2 - Proppant Concentration for the Engram No. 1 Well

The effective propped fracture length for the the Engram No. 1 well was determined to be approximately 1900 ft. For each of the twenty wells studied, the same method of analysis was used to determine both propped fracture length and fracture conductivity.

Once the values of propped fracture length and fracture conductivity for each well were determined from the model PROPTRAN, a computer model called TYPEFIN was used to history match the production data for each of the twenty wells. The computer model TYPEFIN forecasts production from hydraulically fractured wells by using finite conductivity type curves. A summary of the model TYPEFIN and how it was used is presented in Appendix B. The value of fracture length determined from the model PROPTRAN was used in history matching production data. Therefore, the formation permeability was varied until a reasonable match of production data was obtained. In matching production data, cumulative producing time was used. The effects of shut-in periods were not considered. Table 4 shows not only the fracture length determined from the model PROPTRAN but also the formation permeability used in history matching production data using the model TYPEFIN. The Truett No. 1 well was not history matched initially since it only flowed above 300 Mcf/D for two months.

When reviewing the values of formation permeability in Table 4, it is apparent that some of the values are lower than one would expect for a commercial Cotton Valley Lime completion. The fracture lengths also seem rather long. It was assumed that the value of fracture length determined from the model PROPTRAN was correct. Thus, formation

TABLE 4  
Initial Estimates of Fracture Half Length and Formation  
Permeability using Computer Models PROPTRAN and TYPEFIN

Well	Permeability md	Fracture Length ft
Engram No. 1	0.0003	1961
Getty Muse No. 1	0.0045	1000
Vance No. 1	0.0180	1213
McFerran No. 1	0.00019	1000
Hawkins No. 1	0.0100	2100
Muse Duke No. 1	0.0110	2500
Croft No. 1	0.0011	2084
Muse A No. 1	0.0160	846
Webb No. 1	0.0023	1500
Muse Tucker No. 1	0.0034	1860
Presley Sadler No. 1	0.0005	650
Prichard No. 1	0.00054	1254
Kerr No. 1	0.0007	2350
Fenton No. 1	0.00048	1620
Jackson B No. 1	0.0033	1260
Ferguson No. 2	0.0060	1200
Smythe No. 1	0.0016	1290
Renfro No. 1	0.0100	814
Lawrence No. 1	0.0025	1760

permeability was the key variable used in history matching production data. In reviewing the results from the model PROPTRAN, it was evident that the apparent viscosity of the fracture fluid was not correct. The values of  $n'$  (flow behavior index) and  $K'$  (consistency index) that were used in the model were the values reported by service companies several years ago. These values are now known to be optimistic. This caused predicted values of apparent viscosity to be much larger than could actually have been achieved at the time. It is now known that the apparent viscosity of these fluids was about 40-60 cp in the fracture due to shear degradation in the tubing. Therefore, values of  $n'$  and  $K'$  were adjusted such that the apparent viscosity in the fracture was around 40-60 cp.

The fracture treatment data for all 20 wells were then analyzed again using the adjusted values of  $n'$  and  $K'$ . Because of the lower apparent viscosity in the fracture and more proppant settling, the propped fracture length was shorter. Figure 3 illustrates the revised proppant concentration profile for the Engram No. 1 well. The new effective propped fracture length was estimated to be 1300 ft. This is a reduction of 600 ft when compared to the initial fracture length determined with  $n'$  and  $K'$  data supplied by the service companies.

Each well was history matched a second time using the computer model TYPEFIN and the new values of fracture length. Again, formation permeability was the key variable in matching production data. However, the formation permeability used to history match production data was not allowed to be lower than 0.001 md. This was done because it is unlikely

PROPPANT CONCENTRATIONS EXPRESSED IN LB/FT<sup>2</sup>

L E N G T H \* \* F T

0. 384. 768. 1151. 1535. 1919. 2303. 2687. 3070. 3454. 3838.

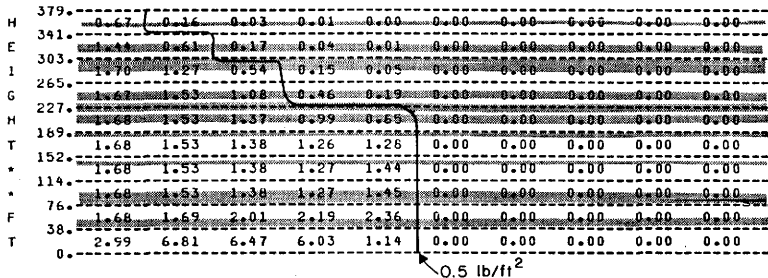


Fig. 3 - Proppant Concentration for the Engram No. 1 Well using Adjusted Values of n' and K'

that a gas well can produce gas in commercial quantities at values of formation permeability below 0.001 md. When the minimum value of formation permeability had to be used, the fracture length was shortened until a reasonable match of production data occurred. Table 5 compares the values of fracture length and formation permeability determined from the model TYPEFIN when using both the service companies' and the adjusted values of  $n'$  and  $K'$ . Figure 4 shows a match of production data using the computer model TYPEFIN. This match of production data is for the Prichard No. 1 well which represents a typical match with the model TYPEFIN. This match was made using a fracture length of 900 ft and a formation permeability of 0.001 md. The match is very good for the first 500 days; however, after this time, the computer model forecasted more production than actually occurred. This difference between the two curves could be caused by liquid loading. The flow rate for the Prichard No. 1 well was approximately 300 Mcf/D when the two curves started to separate.

To refine the values of formation permeability and fracture length determined from the model TYPEFIN, a more sophisticated computer model called FRACSIM was used. This model takes into account fracture closure and non-Darcy flow effects. Appendix C describes the capabilities that the model FRACSIM offers and the data needed to forecast production. When using the model FRACSIM to history match production data, the values of formation permeability and fracture length computed from the model TYPEFIN were used as initial estimates. These values were then adjusted to improve the match of production data. Values of formation

TABLE 5  
 Comparison of History-Matched Parameters With the Computer Model  
 TYPEFIN when using Two Different Sets of Fracture Fluid Data

| Well                 | Service Companies<br>n' and K' |          | Adjusted Values<br>n' and K' |          |
|----------------------|--------------------------------|----------|------------------------------|----------|
|                      | k<br>md                        | xf<br>ft | k<br>md                      | xf<br>ft |
| Engram No. 1         | 0.0003                         | 1961     | 0.0010                       | 975      |
| Getty Muse No. 1     | 0.0045                         | 1000     | 0.0045                       | 1000     |
| Vance No. 1          | 0.0180                         | 1213     | 0.0220                       | 1109     |
| McFerran No. 1       | 0.0002                         | 1000     | 0.0010                       | 380      |
| Hawkins No. 1        | 0.0100                         | 2100     | 0.0130                       | 1500     |
| Muse Duke No. 1      | 0.0110                         | 2500     | 0.0110                       | 2500     |
| Croft No. 1          | 0.0011                         | 2084     | 0.0019                       | 1550     |
| Muse A No. 1         | 0.0160                         | 846      | 0.0160                       | 846      |
| Webb No. 1           | 0.0023                         | 1500     | 0.0023                       | 1500     |
| Muse Tucker No. 1    | 0.0034                         | 1860     | 0.0034                       | 1860     |
| Presley Sadler No. 1 | 0.0005                         | 650      | 0.0010                       | 400      |
| Prichard No. 1       | 0.0005                         | 1254     | 0.0010                       | 900      |
| Kerr No. 1           | 0.0007                         | 2350     | 0.0020                       | 1250     |
| Fenton No. 1         | 0.0005                         | 1620     | 0.0010                       | 1241     |
| Jackson B No. 1      | 0.0033                         | 1260     | 0.0037                       | 1054     |
| Ferguson No. 2       | 0.0060                         | 1200     | 0.0060                       | 1200     |
| Smythe No. 1         | 0.0016                         | 1290     | 0.0016                       | 1290     |
| Renfro No. 1         | 0.0100                         | 814      | 0.0085                       | 985      |
| Lawrence No. 1       | 0.0025                         | 1760     | 0.0025                       | 1760     |
| Average              | 0.0029                         | 1486     | 0.0032                       | 1226     |

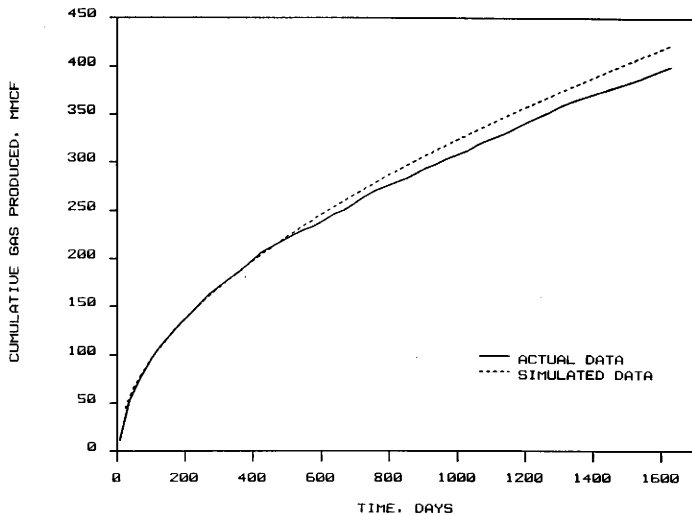


Fig. 4 - History-Match of Production Data for the Prichard No. 1 Well using the Computer Model TYPEFIN for  $K=0.001$  md and  $XF=900$  ft



permeability and fracture length determined with the computer model FRACSIM are shown in Table 6. Because the effects of fracture closure and non-Darcy flow were considered, either the fracture length, formation permeability, or both had to be increased in order to match production data. Figure 5 illustrates the match of production data for the Prichard No. 1 well using the model FRACSIM. The permeability for this well was increased from 0.001 to 0.0012 md. in order to match production data. This resulted in a better match of production data than when using the computer model TYPEFIN.

TABLE 6  
Refinement of History-Matched Parameters using the  
Computer Model FRACSIM

| Well                 | Permeability<br>md | Fracture Length<br>ft |
|----------------------|--------------------|-----------------------|
| Engram No. 1         | 0.0011             | 1000                  |
| Getty Muse No. 1     | 0.0046             | 1000                  |
| Vance No. 1          | * 0.0260           | 1100                  |
| McFerran No. 1       | 0.0010             | 360                   |
| Hawkins No. 1        | * 0.0130           | 1500                  |
| Muse Duke No. 1      | 0.0200             | 2000                  |
| Croft No. 1          | 0.0021             | 1550                  |
| Muse A No. 1         | 0.0160             | 995                   |
| Webb No. 1           | 0.0026             | 1350                  |
| Muse Tucker No. 1    | 0.0040             | 1860                  |
| Presley Sadler No. 1 | 0.0010             | 400                   |
| Prichard No. 1       | 0.0012             | 900                   |
| Kerr No. 1           | 0.0018             | 1250                  |
| Fenton No. 1         | 0.0010             | 1200                  |
| Truett No. 1         | 0.0010             | 250                   |
| Jackson No. 1        | 0.0050             | 1054                  |
| Ferguson No. 2       | 0.0080             | 1250                  |
| Smythe No. 1         | 0.0016             | 1290                  |
| Renfro No. 1         | 0.0140             | 1000                  |
| Lawrence No. 1       | <u>0.0027</u>      | <u>1760</u>           |
| Average              | 0.0035             | 1226                  |

\* Drainage area of 320 acres instead of 640 acres

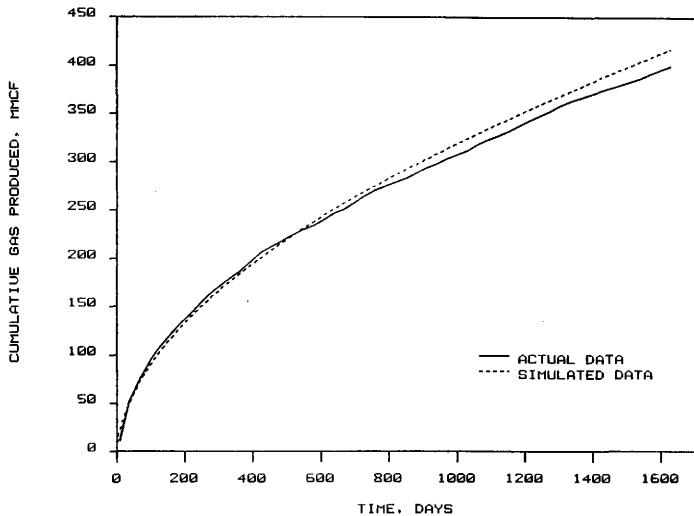


Fig. 5 - History-Match of Production Data for the Prichard No. 1 Well using the Computer Model FRACSIM for  $K=0.0012$  md and  $XF=900$  ft

## CLASSIFICATION OF WELLS

Using the values of fracture length and formation permeability determined from the model FRACSIM, average data sets were determined from the twenty wells which characterized (1) an above average, (2) a below average, and (3) an average well completed in the Cotton Valley Lime. The twenty wells were classified into groups based on their formation permeability. The average logarithmic value of formation permeability for all twenty wells was calculated to be 0.004 md. Using Figure 6, the wells with a formation permeability above 0.01 md were classified as an above average well. Wells with a formation permeability below 0.0015 md were classified as a below average well. The wells between this range were classified as an average well. Figure 6 shows that the data were scattered evenly about a porosity of 6 percent. Therefore, each group was given an average porosity of 6 percent. The formation permeability used for each group was computed as the logarithmic average permeability for the wells in its group. The fracture length and net pay were both calculated as an arithmetic average for the wells in each group.

An average water saturation of 20.5 percent was computed for all twenty wells. When this value of water saturation was used in the average data sets, less than one barrel of water was produced per MMcf of gas. Table 7 shows the cumulative fluid (condensate, gas, and water) production for all twenty wells as of April 1985. The average producing period for these twenty wells was four and a half years. The average

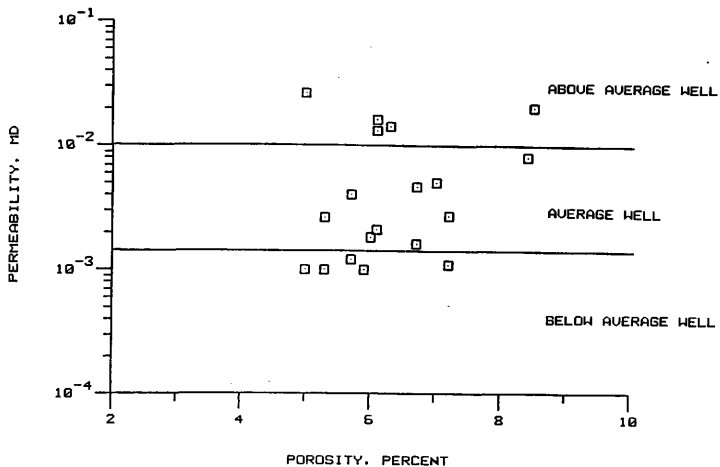


Fig. 6 - Classification of Cotton Valley Lime Wells using Formation Permeability

TABLE 7  
Production Values for the Cotton Valley Lime Wells

| Well                 | Water<br>bbl | Condensate<br>bbl | Gas<br>MMcf | LGR<br>bbl/MMcf |
|----------------------|--------------|-------------------|-------------|-----------------|
| Engram No. 1         | 21452        | 1400              | 641         | 35.6            |
| Getty Muse No. 1     | 8324         | 829               | 906         | 10.1            |
| Vance No. 1          | 17340        | 10710             | 1573        | 17.8            |
| McFerran No. 1       | 11680        | 15                | 522         | 22.4            |
| Hawkins No. 1        | 10020        | 0                 | 1870        | 5.4             |
| Muse Duke No. 1      | 18293        | 0                 | 3634        | 5.0             |
| Croft No. 1          | 5281         | 0                 | 877         | 6.0             |
| Muse A No. 1         | 9027         | 0                 | 2739        | 3.3             |
| Webb No. 1           | 19719        | 0                 | 1062        | 18.6            |
| Muse Tucker No. 1    | 13327        | 0                 | 2223        | 6.0             |
| Presley Sadler No. 1 | 17058        | 3589              | 429         | 48.1            |
| Prichard No. 1       | 5359         | 0                 | 400         | 13.4            |
| Kerr No. 1           | 19215        | 0                 | 651         | 29.5            |
| Fenton No. 1         | 15941        | 1880              | 333         | 53.5            |
| Truett No. 1         | 12663        | 2050              | 232         | 63.3            |
| Jackson B No. 1      | 9985         | 0                 | 2006        | 5.0             |
| Ferguson No. 2       | 8644         | 2995              | 2348        | 5.0             |
| Smythe No. 1         | 18306        | 1355              | 1693        | 11.6            |
| Renfro No. 1         | 6676         | 0                 | 1930        | 3.5             |
| Lawrence No. 1       | 9825         | 0                 | 1540        | 6.4             |
|                      |              |                   | Average     | 18.3            |

liquid-gas ratio (LGR) for these twenty wells is 18.3 bbl/MMcf. The liquid includes both the production of water and condensate. The Truett No. 1 well has the highest LGR of 63.3 bbl/MMcf while the Muse A No. 1 has the lowest LGR of 3.3 bbl/MMcf.

The water production in the Cotton Valley Lime probably comes from thin zones of higher water saturation that are embedded in the total formation. To simulate a layered formation, a three-dimensional model would be necessary. The use of a 3-D model in this case could not be economically justified. Therefore, to simulate the correct amount of liquid production, the water saturation in the two-dimensional model was increased to allow for more liquid flow. In other words, the water saturation was increased until a LGR of 3 bbl/MMcf was achieved when using an extremely low relative permeability to water curve. Therefore, when a more optimistic relative permeability to water curve is used, the LGR will be higher and the range of liquid-gas ratios which occurs in the field will also occur in the three average data sets. This resulted in increasing the water saturation from 20.5 to 40 percent. To account for the increase in water saturation, the total porosity was increased to 7.95 percent so that the gas-in-place remained unchanged. Table 8 shows the parameters that were varied for each individual group and also the parameters that were held constant.

TABLE 8  
Average Reservoir Properties Characterizing  
the Cotton Valley Lime

Original Pressure = 6300 psi  
 Average Water Saturation = 40.0%  
 Total Porosity = 7.95%  
 Reservoir Temperature = 285pF  
 Bottom-hole Treating Pressure = 8100 psi  
 Fracture Permeability = 3.5 E05 md  
 Fracture Fluid Volume = 10,000 bbls

|                     | <u>ABOVE AVERAGE</u> | <u>AVERAGE</u> | <u>BELOW AVERAGE</u> |
|---------------------|----------------------|----------------|----------------------|
| Net Pay, ft         | 40                   | 65             | 90                   |
| Permeability, md    | 0.017                | 0.003          | 0.001                |
| Fracture Length, ft | 1300                 | 1300           | 750                  |



## ANALYSIS OF LIQUID LOADING

The average data sets determined from the twenty Cotton Valley Lime wells were used to study the liquid loading problem using a two-phase, two-dimensional computer model called GASWAT. More information about the model GASWAT is given in Appendix D. In analyzing the liquid loading problem, a sensitivity study was conducted to see what effect certain parameters had on long term production. The parameters that were investigated were the effects of (1) relative permeability to water, (2) relative permeability to gas, (3) gas permeability hysteresis, (4) capillary pressure, and (5) formation damage.

### Relative Permeability Functions

In studying the flow of both gas and water in porous media, relative permeability and capillary pressure curves had to be obtained. Figure 7 shows the relative permeability to gas (KRG) curves which were used in this study. The KRG1 curve is a gas relative permeability curve taken from a Cotton Valley Lime core under in-situ conditions. The KRG2 curve is a gas relative permeability curve for an Edwards Limestone core. This is a limestone reservoir which has similiar characteristics to the Cotton Valley Lime. The KRG3 curve is the gas relative permeability curve used in the study by Holditch.<sup>9</sup> The relative permeability to water (KRW) curves are shown in Figure 8. The KRW1 curve is the water relative permeability curve for the Edwards Limestone core. This is the same KRW curve used in the study by Holditch.<sup>9</sup> Since there were no relative permeability to water data for the Cotton Valley

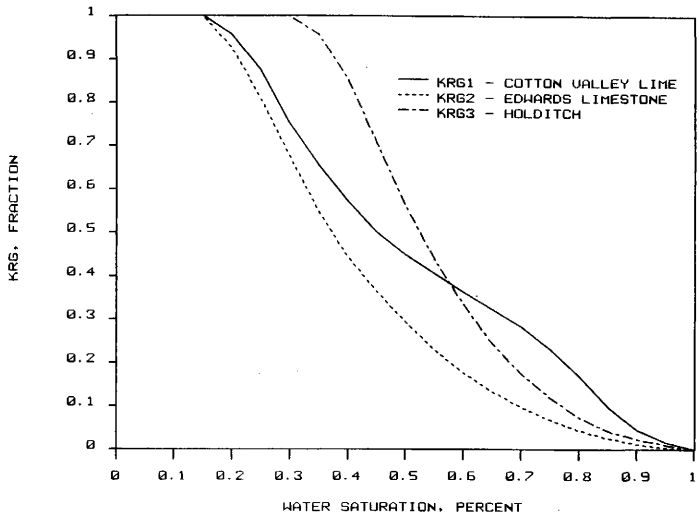


Fig. 7 - Gas Relative Permeability Curves used in Analysis of Liquid Loading

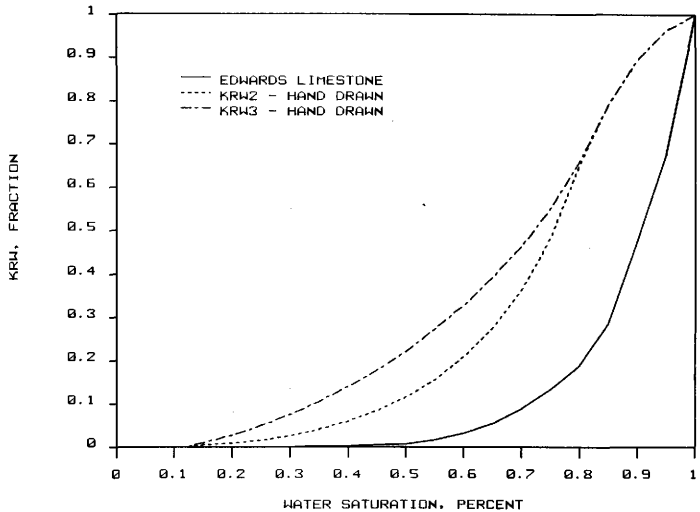


Fig. 8 - Water Relative Permeability Curves used in Analysis of Liquid Loading

Lime, two other KRW curves were used to study the effect of relative permeability to water. The KRW2 and KRW3 curves are not actual laboratory relative permeability curves, but are hand drawn curves. These two curves were drawn to investigate the effects of water mobility in the reservoir upon the liquid loading problem.

#### Capillary Pressure Functions

Capillary pressure curves are difficult to measure in the Cotton Valley Lime due to the low formation permeability and the time required to obtain the data. Since there were no capillary pressure data available for the Cotton Valley Lime, three different tight gas capillary pressure curves were used to determine what effect capillary pressure had upon long term production. Figures 9 and 10 present the capillary pressure curves for an Edwards Limestone core and a tight gas sandstone core sample, respectively. Figure 11 is not a actual laboratory capillary pressure curve, but an average capillary pressure curve drawn after reviewing capillary pressure data for many tight gas reservoirs.

#### The Fracture

A successful hydraulic fracture treatment results in a fracture with a high permeability. The mobilities of both the gas and liquid are substantially higher in the fracture than in the reservoir due to the contrast in permeability between the fracture and the reservoir. The gas flow in the fracture will generally be turbulent due to the high producing rates, low gas viscosity, and the high permeability in the fracture. Therefore, non-Darcy flow is considered in the fracture.

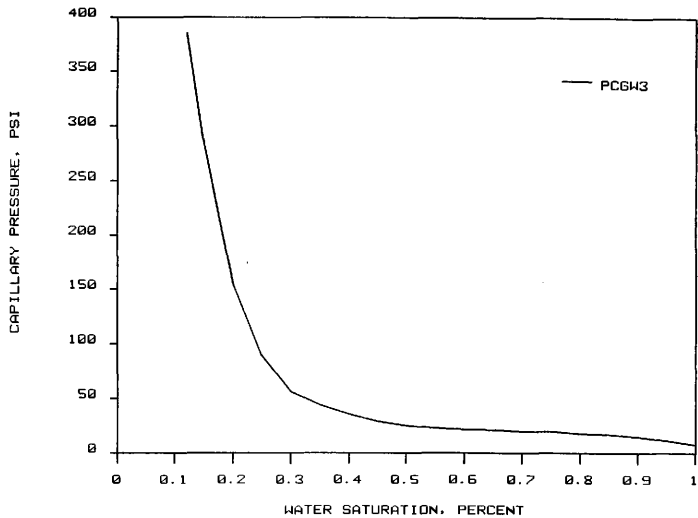


Fig. 9 - Capillary Pressure Curve for an Edwards Limestone Core Sample with a Porosity of 5.9% and a Permeability of 0.12 md

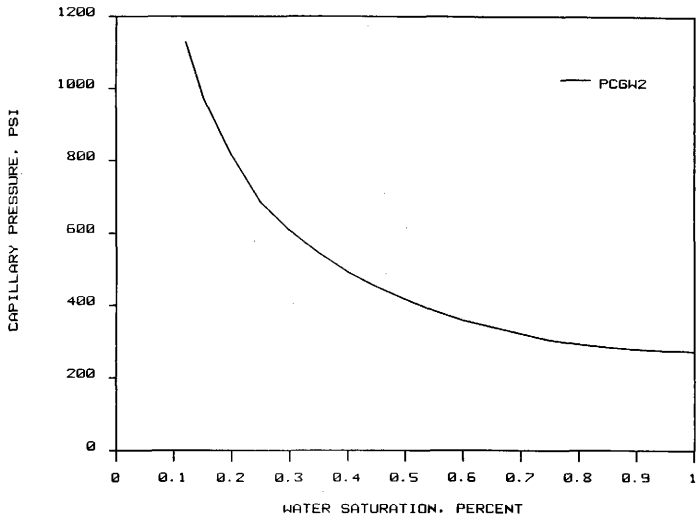


Fig. 10 - Capillary Pressure Curve for a Tight Gas Sandstone Core Sample with a Porosity of 10% and a Permeability of 0.0017 md

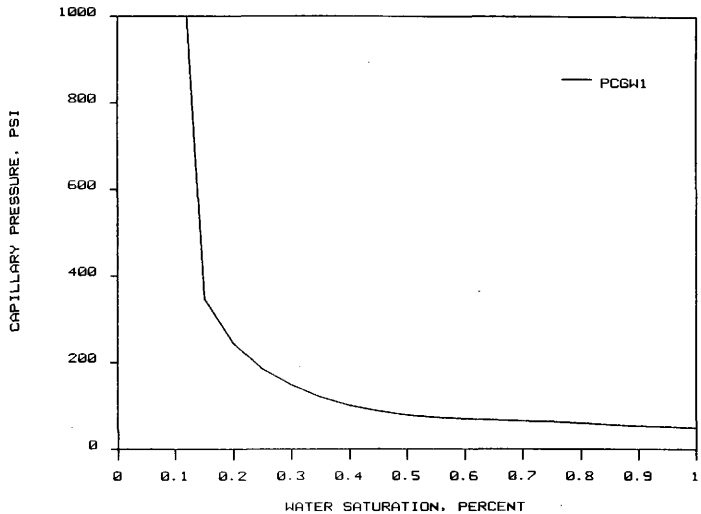


Fig. 11 - Capillary Pressure Curve Which Represents an Average Tight Gas Core Sample with a Porosity of 8% and a Permeability of 0.01 md

In modeling the fracture, the gas and liquid pressures are equal at each point in the fracture since the capillary forces are negligible in a pack of relatively uniform sized proppant particles. The fluid flow in the fracture assumes straight-line relative permeability curves. This is equivalent to complete segregation and appears valid due to the high permeability in the fracture.

#### The Saturated Region

To study the liquid loading problem, a saturated region, which was due to the fracture fluid pumped into the reservoir, was placed around the fracture, as shown in Figure 12. The grid pattern presented in Figure 13 was used to model the saturated region. Table D-4, Appendix D, contains the grid dimensions which were used to model the fracture, the saturated region, and the undamaged reservoir. The saturated region contained the 10,000 barrels of fracture fluid. The fracture fluid was placed around the fracture such that a smooth saturation gradient existed between the fracture and the undamaged reservoir.

#### Production Runs and Injection Runs

Two different computer runs were made for each parameter investigated to determine the effects of the injected fracture fluids on long term production. One run placed the injected fracture fluids in and around the fracture. The fracture was initially filled with the injected fluids, and the remaining fluids were distributed in the saturated region such that a smooth saturation gradient existed between the fracture and the undamaged reservoir. This type of run represents



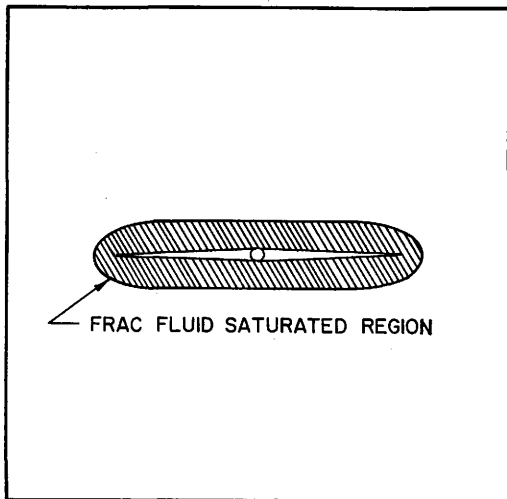


Fig. 12 - Areal View of Drainage Area

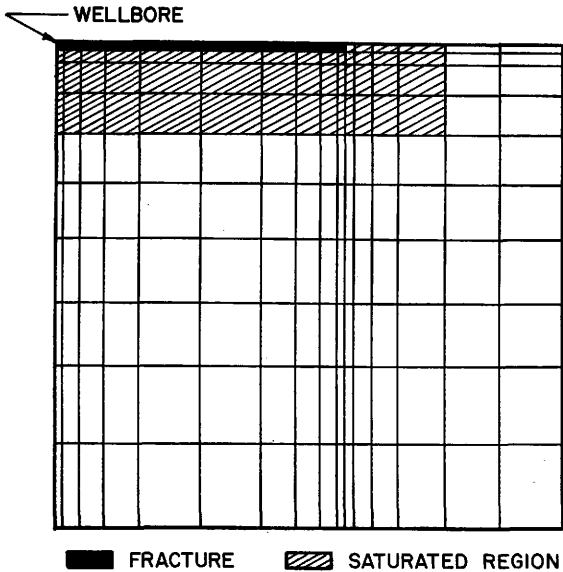


Fig. 13 - Grid Pattern used to Model 1/4 of the Drainage Area using the Computer Model GASHAT

the actual production process that occurs in the field and will be called an injection run to aid in discussing the results.

The second run made for each parameter did not consider the injected fracture fluids. Instead, it represented the ideal case in which the fracture was created without the injection of any fracture fluid. Therefore, no saturated region existed in this run. This type of run will be called a production run in discussing the results.

Long term production will be defined in this study as twenty years of gas production, and short term production will be defined as one year of gas production.

#### Effect of Various Parameters on Long Term Production

##### Effect of Relative Permeability to Water

The average Cotton Valley Lime data set was used to study the effect of relative permeability to water on long term production. For this investigation, the relative permeability to gas and the capillary pressure were held constant for each of the three different relative permeability to water curves. The cumulative gas produced using the three different KRW curves is presented in Figure 14. The gas production after twenty years is lower when the KRW1 relative permeability to water curve was used. The KRW1 curve represents the case where the fracture fluid is immobile and remains around the fracture. Figure 15 illustrates the cumulative water production for each of the three injection runs. It shows that more water was produced when a more optimistic KRW curve was used. Although more water was produced when using a more optimistic relative permeability to water

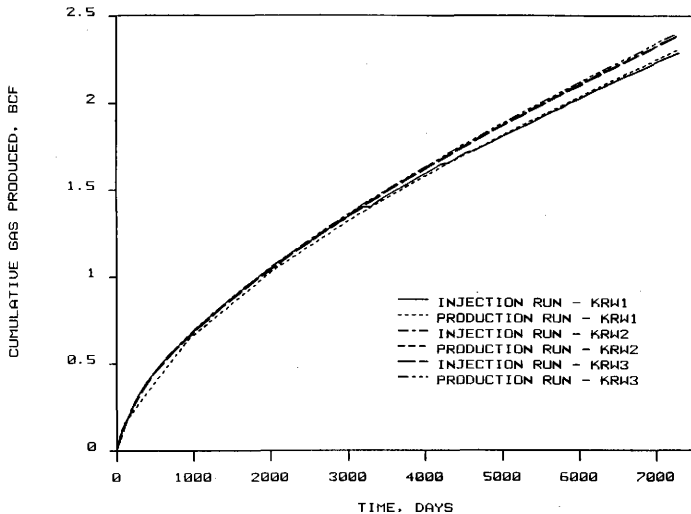


Fig. 14 - Effect of Relative Permeability to Water on Long Term Production using the Average Cotton Valley Lime Data Set for KR61 and PC61 Curves

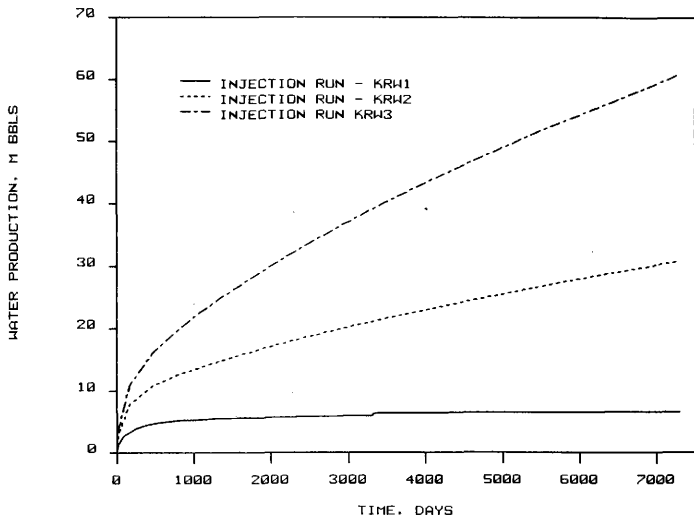


Fig. 15 - Effect of Relative Permeability to Water on Water Production using the Average Cotton Valley Lime Data Set for KR61 and PC6W1 Curves

curve, there was no incremental increase in gas production when the fracture fluid is mobile. This is depicted by the production and injection runs for the KRW2 and KRW3 curves shown in Figure 14. Figure 16 presents the water production for both the production and injection run when using the KRW3 relative permeability to water curve. It shows that the incremental increase in water production was due to the fracture fluid that initially occupied the saturated region. Also, the difference in gas production between the production and injection run for either one of the KRW curves is very small. This is illustrated in Figure 14. In conclusion, there will be a decrease in gas production if the fracture fluid is immobile and remains next to the fracture. However, if the fracture fluid is mobile, the relative permeability to water will only affect water production and have no effect on gas production.

#### Effect of Relative Permeability to Gas

The relative permeability to gas was investigated using the average Cotton Valley Lime data set. This was accomplished by using the same relative permeability to water and capillary pressure curves throughout this part of the investigation. The KRG curves in Figure 7 had to be normalized in order to investigate the effect that relative permeability to gas has on long term production. If the KRG curves had not been normalized, more gas would have been produced when using a more optimistic KRG curve simply because it provided a higher gas permeability in the undamage reservoir. Therefore, the three KRG curves were normalized to a KRG of 1.0 at the initial water saturation of 40

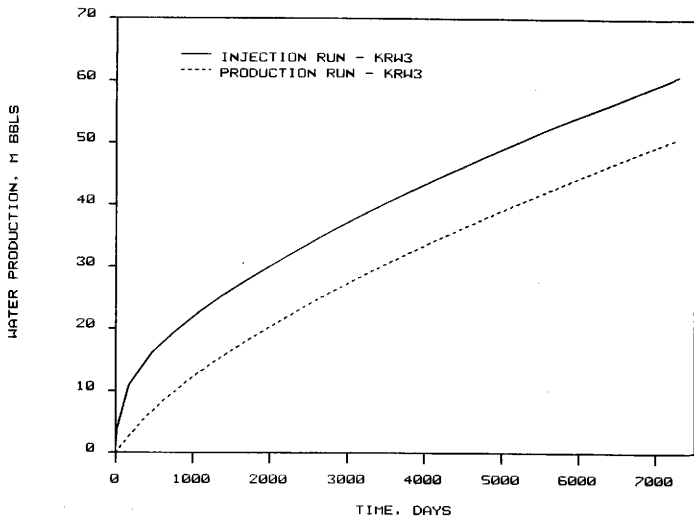


Fig. 16 - Effect of Saturated Region on Water Production using the Average Cotton Valley Lime Data Set for KR61 and PC6H1 Curves

percent. The normalized relative permeability to gas curves are presented in Figure 17. Since the normalized KRG3 curve falls in between the normalized KRG1 and KRG2 curves, only the normalized relative permeability to gas curves NKRG1 and NKRG2 were used. Figure 18 shows the effect that relative permeability to gas has on long term production when using the normalized KRG curves. As illustrated in the figure, the shape of the relative permeability to gas curve has very little effect on long term production and the liquid loading problem.

#### Effect of Gas Permeability Hysteresis

The average Cotton Valley Lime data set was used to study the effect of gas permeability hysteresis. The capillary pressure was held constant, and the KRW1 and KRW3 relative permeability to water curves were used to see if the rate at which the water was removed from the saturated region had any effect upon gas production. The KRW1 curve represents the case where the fracture fluid is immobile and remains next to the fracture, while the KRW3 curve represents the case where the fracture fluid is mobile. To study the effects of gas permeability hysteresis, four different cases were investigated. The first three cases had the effects of gas permeability hysteresis starting at the initial water saturation of 40 percent. These three cases had an irreducible gas saturation of 22, 33, and 40 percent, respectively. The irreducible gas saturation was calculated using Eqs. 2 and 3.

$$C4 = \left[ \frac{1}{SGHYS - DSGHYS} \right] - \left[ \frac{1}{1 - SWR} \right] \dots \dots \dots (2)$$



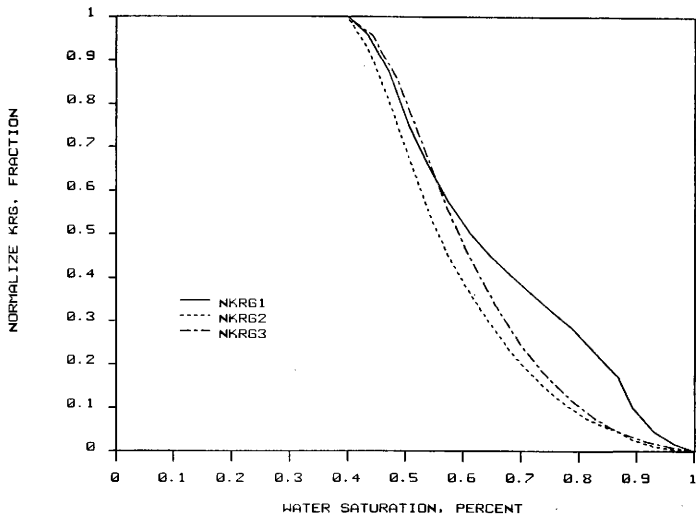


Fig. 17 - Normalized Relative Permeability to Gas Curves used in the Analysis of Liquid Loading

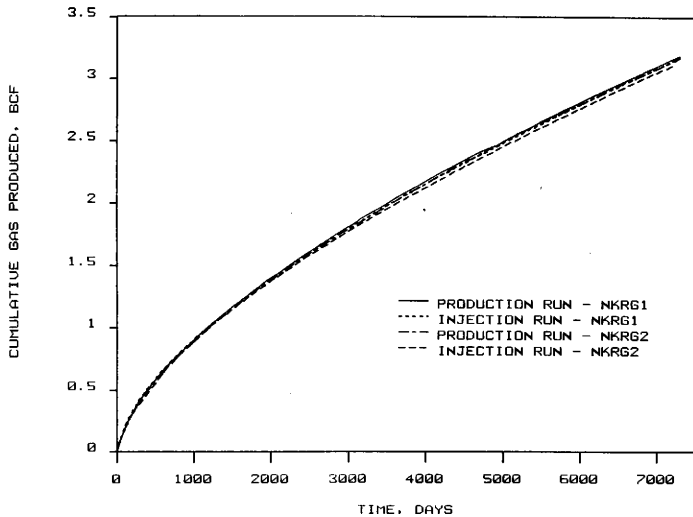


Fig. 18 - Effect of Relative Permeability to Gas on Long Term Production using the Average Cotton Valley Lime Data Set for KR61 and PC61 Curves

$$\text{SGR} = \frac{\text{SGHYS}}{1 + C^4 \text{SGHYS}} \dots \dots \dots (3)$$

The terms which are used to calculate the irreducible gas saturation are defined in Figure 19. The fourth case started the effects of gas permeability at a water saturation of 20 percent and had an irreducible gas saturation of 40 percent. The formation permeability in the undamaged reservoir was increased for the fourth case so that the effects of gas permeability hysteresis only occurred in the saturated region. Two different runs were made for each relative permeability to water curve using different degrees of gas permeability hysteresis. The gas permeability hysteresis was calculated using Killough's method.<sup>14</sup>

$$\text{KRG} = \text{RKHYS} * \left[ \frac{1 - \text{SW} - \text{SGR}}{\text{SGHYS} - \text{SGR}} \right]^{\text{LAMDA}} \dots \dots \dots (4)$$

The degree of gas permeability hysteresis is controlled by using different values of LAMDA. Hysteresis causes a change in permeability due to a change in the saturation history of the reservoir rock. The gas permeability decreases in this situation due to the imbibition of the fracture fluid into the saturated region. Figure 19 demonstrates the effect of using a LAMDA of 1 and 2. Two different sets of runs were made using a LAMDA of 1 and 2.

Figure 20 illustrates the relative permeability to gas curves with hysteresis included when using a LAMDA of 1. The effects of gas permeability hysteresis when using the KRW3 relative permeability to

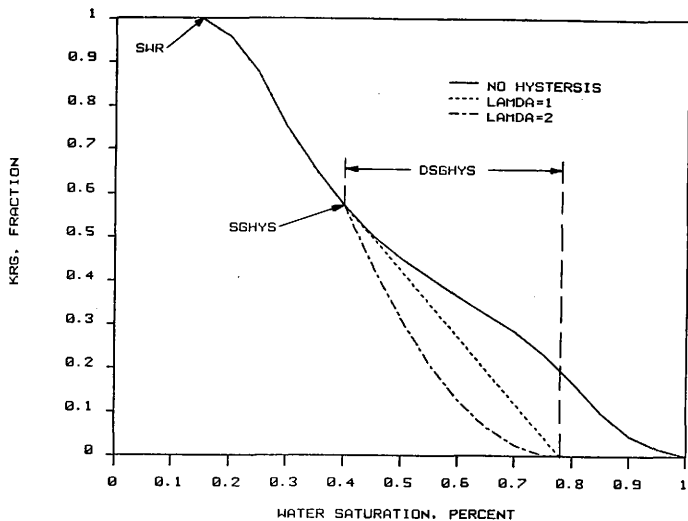


Fig. 19 - Effect of the Parameter LAMDA on Gas Permeability Hysteresis when using the Killough Method

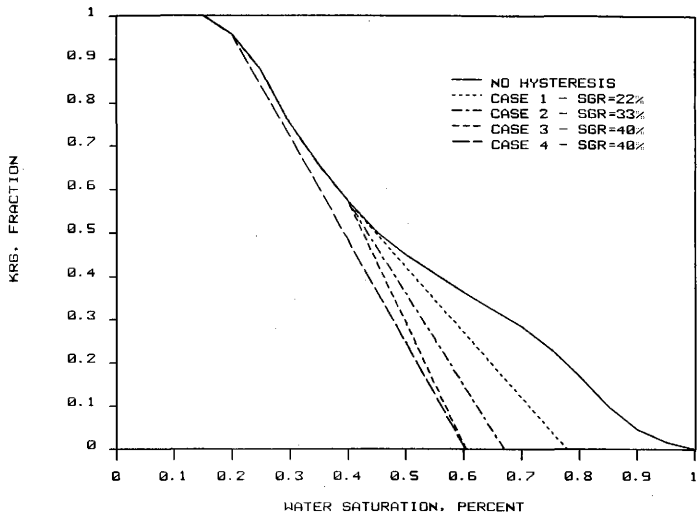


Fig. 20 - Effect of Hysteresis on Relative Permeability to Gas when using a Lambda of 1

water curve is presented in Figures 21 and 22. Figure 21 shows the gas permeability hysteresis effects after one year of production, while Figure 22 shows the effects of gas permeability hysteresis after 20 years of production. There is a little difference in production after one year; however, there is no difference in production after 20 years.

Figure 23 presents the effects of gas permeability hysteresis on one year of gas production when using the KRW1 relative permeability to water curve, while Figure 24 shows the gas permeability hysteresis effects over 20 years of production. Again, gas permeability hysteresis has no effect on long term production. However, there is a larger difference in gas production after one year as illustrated by Figure 23.

In Figure 23, Cases 3 and 4 produced only water for the first two weeks. This represents a long period of time following a hydraulic fracture treatment before gas production begins. In the industry, if there had been no gas production in the first two weeks following a hydraulic fracture treatment, the well would probably have been abandoned. It would have been concluded that the fracture treatment was not properly designed or that the fracture had grown into a water bearing formation. A pre-fracture analysis done prior to the fracture treatment would be helpful in determining whether the conclusions for abandoning the well are justified. This adds to the importance of why a thorough pre-fracture analysis should be done prior to a hydraulic fracture treatment. However, if the well had not been abandoned, gas production would have begun after the second week. The difference in gas production after one year between Cases 3 and 4 and the case where

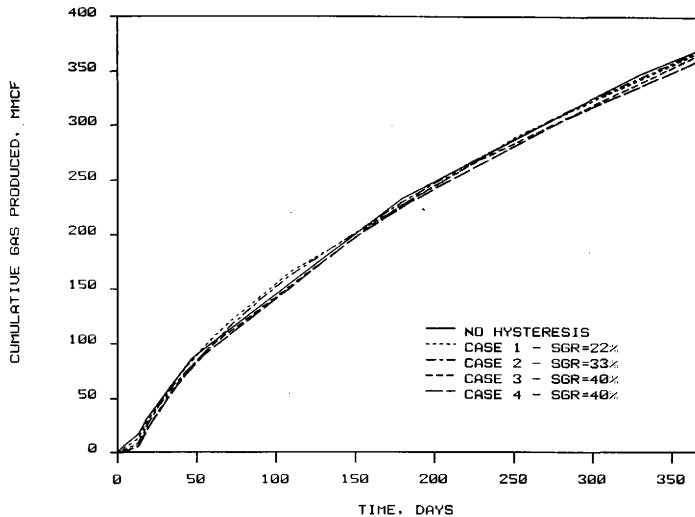


Fig. 21 - Effect of Gas Permeability Hysteresis on Short Term Production using the Average Cotton Valley Lime Data Set for LAMDA of 1 and KR61, KR43, and PC641 Curves.

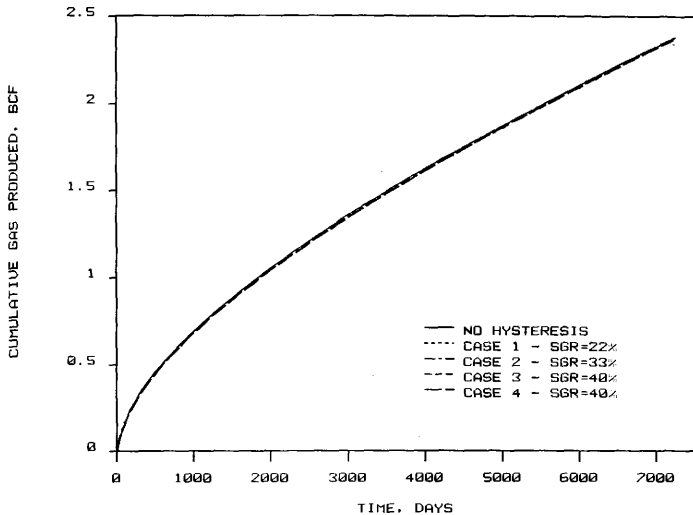


Fig. 22 - Effect of Gas Permeability Hysteresis on Long Term Production using the Average Cotton Valley Lime Data Set for LAMDA of 1 and KR61, KRW3, and PCGH1 Curves



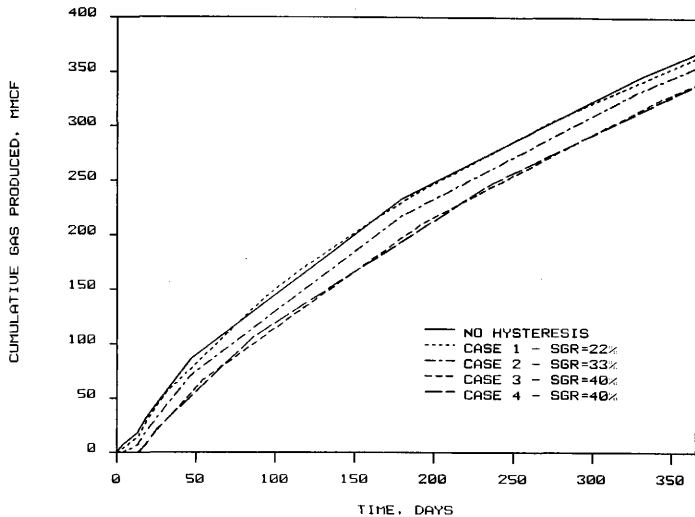


Fig. 23 - Effect of Gas Permeability Hysteresis on Short Term Production using the Average Cotton Valley Lime Data Set for LANDA of 1 and KRG1, KRH1, and PCBH1 Curves

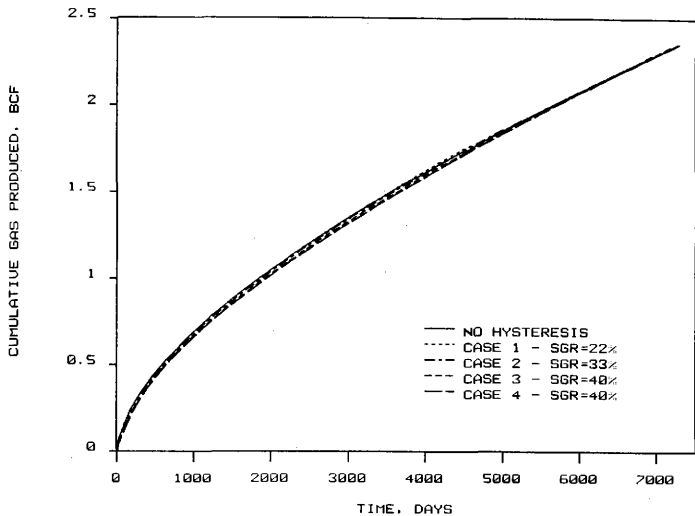


Fig. 24 - Effect of Gas Permeability Hysteresis on Long Term Production using the Average Cotton Valley Lime Data Set for LAMDA of 1 and KRGI, KRHI, and PCGW1 Curves

hysteresis was neglected would be only 8 percent, and there would be no difference in long term production as illustrated in Figure 24. Therefore, it may take some wells longer to cleanup following a hydraulic fracture treatment due to gas permeability hysteresis and the fracture fluid remaining immobile next to the fracture. However, this showed only minor effects on long term production.

The second set of runs were made with a LAMDA of 2. The gas permeability hysteresis curves are presented in Figure 25 for a LAMDA of 2. When using the KRW3 relative permeability to water curve, the effect of gas permeability hysteresis on long term production was negligible, as illustrated in Figure 26. Figure 27 illustrates the effects of gas permeability hysteresis on production after one year. The difference in gas production is much greater than when LAMDA was equal to 1. Figure 28 shows the effects of gas permeability hysteresis on production after 20 years when using the KRW1 relative permeability to water curve. This figure illustrates that in this case, the gas permeability hysteresis affected long term production. For example, to produce 2 Bcf of gas it would take 5645 days when hysteresis was neglected, and it would take 6000 days for Case 4 where hysteresis was included. This is a difference of 355 days.

Figure 29 presents the gas permeability hysteresis effects on production after one year. Case 2 produced only water for the first two weeks. And Cases 3 and 4 only produced water for the first three weeks. In the field, it is very unlikely that a well would be swabbed for three weeks if it has just been hydraulically fractured. Instead, the well

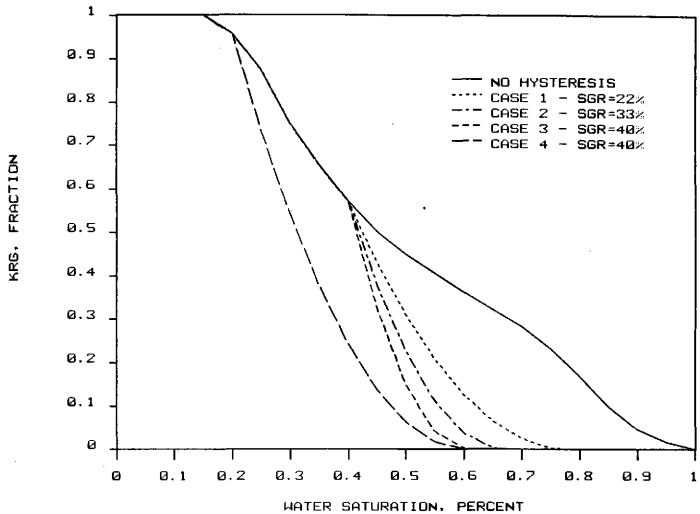


Fig. 25 - Effect of Hysteresis on Relative Permeability to Gas when using a LAMDA of 2

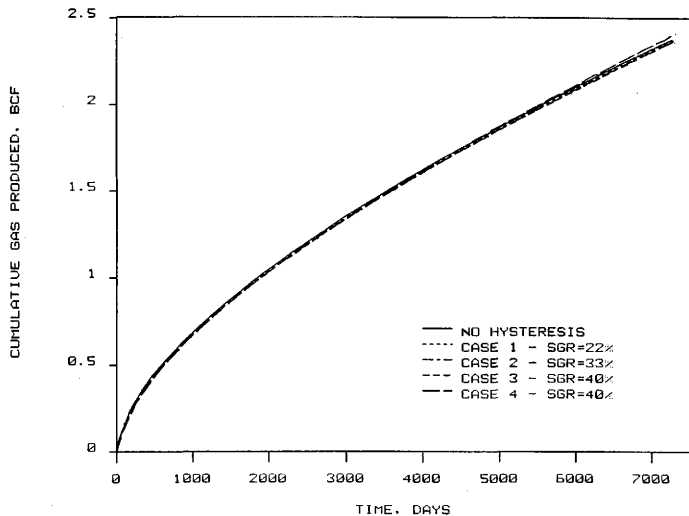


Fig. 26 - Effect of Gas Permeability Hysteresis on Long Term Production using the Average Cotton Valley Lime Data Set for  $\lambda_{MDA}$  of 2 and KR61, KR43, and PC641 Curves

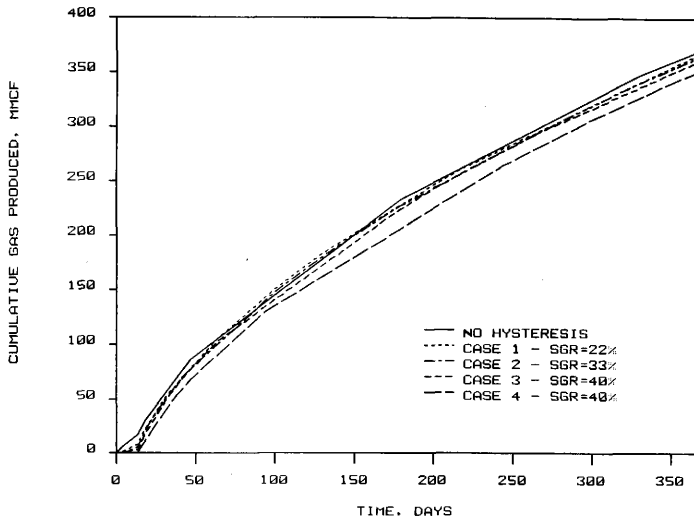


Fig. 27 - Effect of Gas Permeability Hysteresis on Short Term Production using the Average Cotton Valley Lime Data Set for  $\lambda_{MO}$  of 2 and KRG1, KRW3, and PCW1 Curves

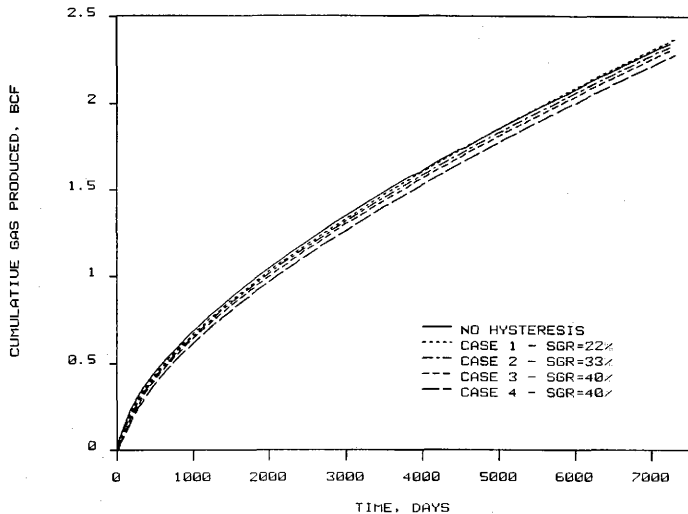


Fig. 28 - Effect of Gas Permeability Hysteresis on Long Term Production using the Average Cotton Valley Lime Data Set for LAMDA of 2 and KRGI, KRNI, and PCGI Curves

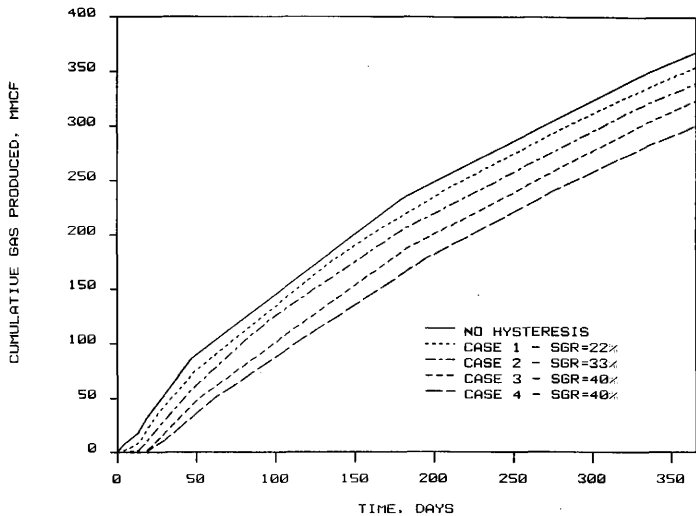


Fig. 29 - Effect of Gas Permeability Hysteresis on Short Term Production using the Average Cotton Valley Line Data Set for LAMDA of 2 and KR61, KR41, and PC61 Curves



would probably be abandoned and its failure blamed on the designed of the fracture treatment. However, if the well was not abandoned, there would be an 18 percent difference in gas production between Case 4 and the case where gas permeability hysteresis was neglected after one year. This is an additional decrease in gas production of 10 percent compared to when LAMDA was equal to 1. The difference in long term production between these two cases is only 3 percent. The results concerning the effect of gas permeability hysteresis indicate that cumulative gas production after twenty years will be affected if the fracture fluid remains immobile next to the fracture and the irreducible gas saturation is greater than 30 percent. However, the gas production after one year will be affected by gas permeability hysteresis as reported by previous research.<sup>9</sup> Also, the cleanup period following a hydraulic fracture treatment can last for several weeks due to the effects of gas permeability hysteresis. This stresses the importance of a complete pre-fracture analysis before a hydraulic fracture treatment.

#### Effect of Capillary Pressure

The average Cotton Valley Lime data set was used to study the effect of capillary pressure on long term production and the liquid loading problem. The relative permeability to gas and water were held constant throughout this study. The effect of varying degrees of capillary pressure were compared to the ideal case in which capillary pressure was neglected. The effect capillary pressure has on long term production is presented in Figure 30. The difference between cumulative gas production when using either the Edwards Limestone (PCGW3) or the

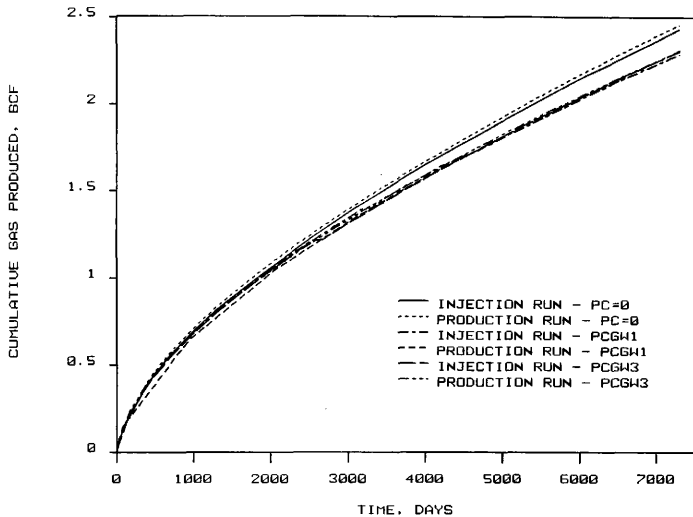


Fig. 30 - Effect of Capillary Pressure on Long Term Production using the Average Cotton Valley Lime Data Set for KRG1 and KRH1 Curves

average capillary pressure (PCGW1) curve was negligible. However, the cumulative gas production was higher when capillary pressure was neglected. The difference between gas production when using and neglecting capillary pressure was 5 percent. Since there was little difference in long term production when using either the Edwards Limestone or the average capillary pressure curve, the tight gas sandstone capillary curve was used in which the capillary pressure was doubled to see if a higher displacement pressure would have any effect on ultimate recovery. Figure 31 shows the effect of using displacement pressures of 275 and 550 psi. There was only a two percent decrease in gas production when the displacement pressure was increased from 275 to 550 psi. It is apparent from Figures 30 and 31, that as long as there is some capillary pressure, gas production will decrease by 5 percent.

#### Effect of Formation Damage

To determine what effect formation damage has on long term production, the average Cotton Valley Lime data set was used. The relative permeability and capillary pressure curves were held constant for this study so that only the effect of formation damage was investigated. The formation damage, which was due to rock deformation and adverse reaction between the formation and fracture fluids, was limited to the areal extent of the saturated region, as shown in Figures 12 and 13. Two different computer runs were made in which formation damage was included in the saturated region. The formation permeability in the saturated region for the two computer runs was reduced from 0.003 md to 0.0015 md and 0.0003 md, respectively. Figure 32 illustrates the

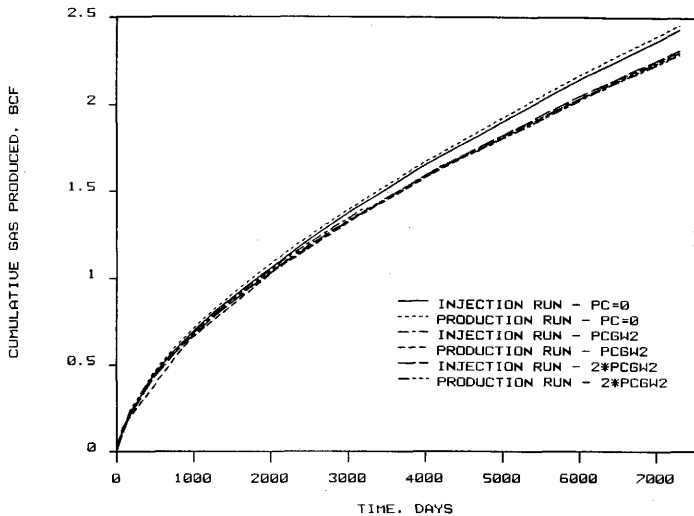


Fig. 31 - Effect of Displacement Pressure on Long Term Production using the Average Cotton Valley Lime Data Set for KR61 and KR41 Curves

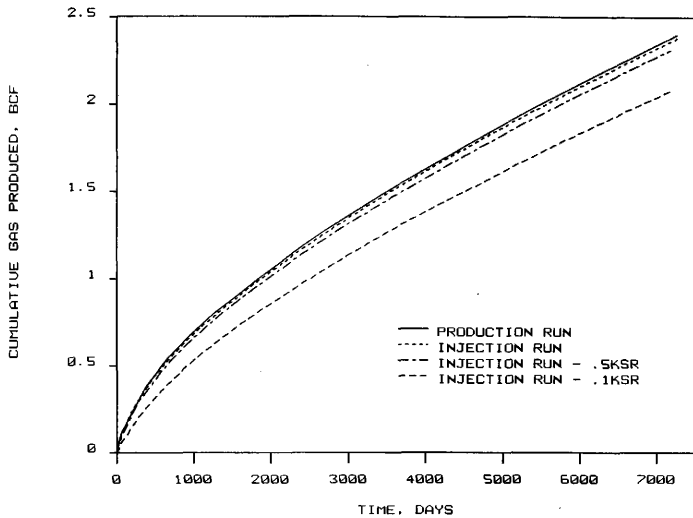


Fig. 32 - Effect of Formation Damage on Long Term Production using the Average Cotton Valley Lime Data Set for KR61, KR43, and PC6W1 Curves

effect that formation damage has on long term production. Gas production was reduced by 3 percent when the formation permeability around the fracture was reduced by 50 percent. However, a 13 percent reduction in gas production occurred when the formation permeability was reduced by an order of magnitude. This indicates that the effect of formation damage will be negligible unless the formation permeability in the saturated region is reduced by an order of magnitude or more.

#### Calibrating the Reservoir Model for Liquid Loading

The production data for the Prichard No. 1 well was history matched with the model GASWAT to verify that the model could actually simulate the liquid loading that occurs in the field. Figure 5 shows the history-match of production data for the Prichard No. 1 well when using the single-phase model FRACSIM. After 600 days of production, the model FRACSIM predicted more gas production than actually occurred in the field. It was believed that the two curves separate after 600 days of production because the well loading up with liquids. This could not be accounted for by the model FRACSIM.

Only the first 200 days of production could be history match for the Prichard No. 1 well when using the model GASWAT, as shown in Figure 33. The match of production data for the Prichard No. 1 well was better when the single-phase model FRACSIM was used. In reviewing the results from the model GASWAT, water was continuously produced at gas flow rates below 300 Mcf/D. The model GASWAT did not load up with liquids at low gas flow rates as occurs in the field. Instead, it produced all the

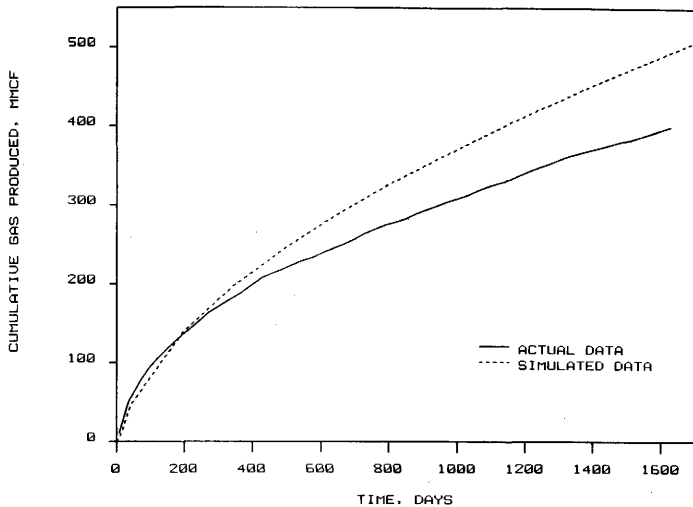


Fig. 33 - History-Match of Production Data for the Prichard No. 1 Well using the Computer Model GASHAT for  $K=0.0017$  md and  $X_F=900$  ft

water that reached the wellbore. This was because the model neglects fluid flow in the tubing.

To account for the flow of fluids in the tubing, a parameter called QMIN was included into the model GASWAT. The parameter QMIN, which is analogous to the minimum or critical gas velocity, was defined as the critical gas flow rate required for continuous removal of all the liquid out of the wellbore. If the gas flow rate is higher than this critical gas flow rate, all the water entering the wellbore will be removed. Thus, no liquid loading problem results. However, once the gas flow rate in the tubing drops below the critical gas flow rate, the model will not allow water to be removed from the wellbore. The water is not allowed to be removed because the gas flow rate can not efficiently lift the liquid out of the wellbore. This leads to increased water saturation in the fracture and the matrix blocks surrounding the fracture. Eventually, the water fills up the fracture, and the gas production drops to zero. At this time, the model is shut in to allow the pressure around the wellbore to build up. When the pressure near the wellbore has increased sufficiently, the well is brought back on line, and both gas and water are produced. This sequence of shutting the well in to allow the pressure to build up is analogous to actual field practices, a practice that is often called stopcocking.

Using the QMIN parameter, the Prichard No. 1 well was history matched a second time using the model GASWAT. The value of QMIN was varied until a reasonable match of production data occurred. Figure 34 presents the history-match of production data for three different values



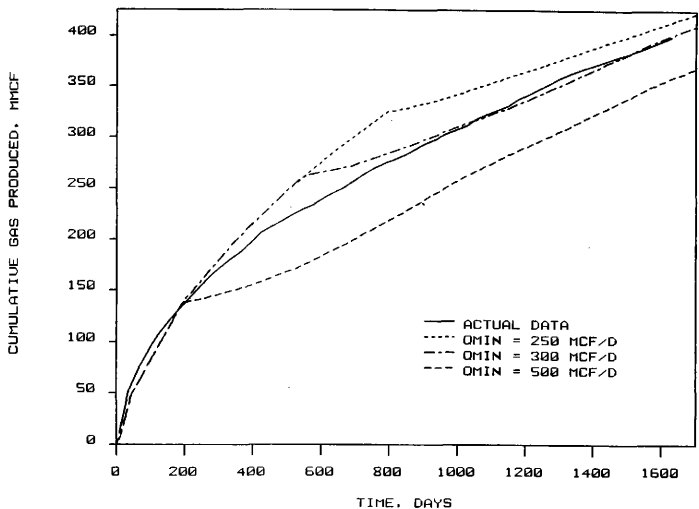


Fig. 34 - History-Match of Production Data for the Prichard No. 1 Well using Different Values of OMIN and the Computer Model GASHAT for  $K=0.0017$  md and  $Xf=900$  ft

of QMIN. It shows that a low value of QMIN will result in more gas production, while a high value of QMIN will result in less gas production. The best match of production data was obtained when QMIN was 300 Mcf/D. This is the same flow rate at which the single-phase model FRACSIM began to diverge from the actual data in Figure 5. Although a QMIN of 300 Mcf/D gave the best match of production data, the results did not closely match the field data between 250 and 850 days. The reason the model did not match the production data during this period was because the model GASWAT does not consider the different flow regimes which occur in the tubing. Instead, it assumes that the water is either flowing or not flowing up the tubing. This was why the simulated data only match the beginning and ending portions of the production data. Figure 35 shows the history-match of water produced when using a QMIN of 300 Mcf/D. The match is acceptable considering that the different flow regimes in the tubing were neglected. Also of importance was the fact that the KRW3 relative permeability to water curve had to be used to produce this much water. This curve was considered an optimistic KRW curve, and all research done in the past has used a KRW curve similar to the KRW1 curve. It is clear from the history-match of the Prichard No. 1 well that the model GASWAT using the critical gas flow rate, QMIN, does model the liquid loading that occurs in the field.

#### Effect of Liquid Buildup In and Around the Fracture

In the history-match of production data for the Prichard No. 1 well, there was a single value of QMIN which gave the best match of

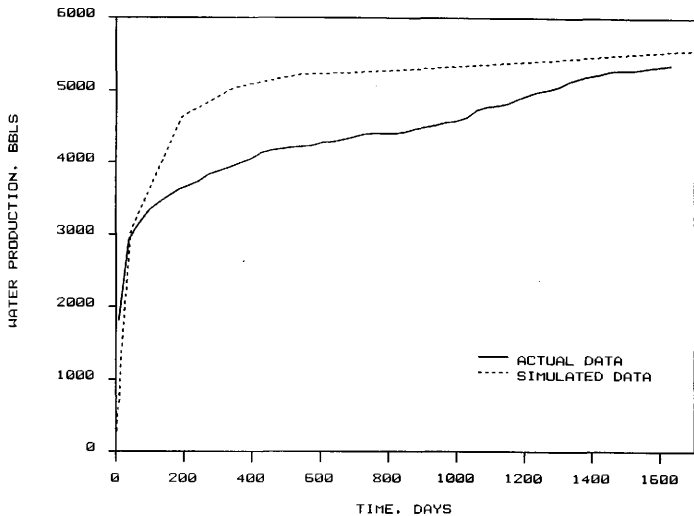


Fig. 35 - History-Match of Water Production for the Prichard No. 1 Well using the Computer Model GASHAT for  $K=0.0017$  md and  $XF=900$  ft

production data. As shown in Figure 34, this value was 300 Mcf/D. This verified that the computer model GASWAT could model the liquid loading that occurs in these Cotton Valley Lime gas wells. However, it also brought up a question as to what effect QMIN has on long term production.

To determine the effect that QMIN has on long term production, the capillary pressure and relative permeability curves were held constant while three different cases were investigated. A different value of QMIN was used in each case to show the effect of QMIN on long term production. The first case, which was considered the ideal case, had a QMIN of 0 Mcf/D. This inferred that all the water would be produced from the wellbore independent of the gas flow rate. Cases 2 and 3 had values of QMIN of 300 and 500 Mcf/D, respectively. The below average Cotton Valley Lime data set was used for all three cases. Figure 36 shows the effect of QMIN on long term production. The cumulative gas production for Case 2 matches the ideal case for the first 1250 days, while Case 3 only matches the first 500 days. This occurs because Case 3 starts loading up with liquids sooner due to the higher value of QMIN. However, at 3800 days the cumulative gas production is the same for Cases 2 and 3. Also, Cases 2 and 3 have almost the same production history after 3800 days.

It is also important to notice that the curves which model the liquid loading, Cases 2 and 3, have the same slope as the ideal case. They are just offset by a time increment. This means it will just take a longer period of time to recover the same amount of gas had there been

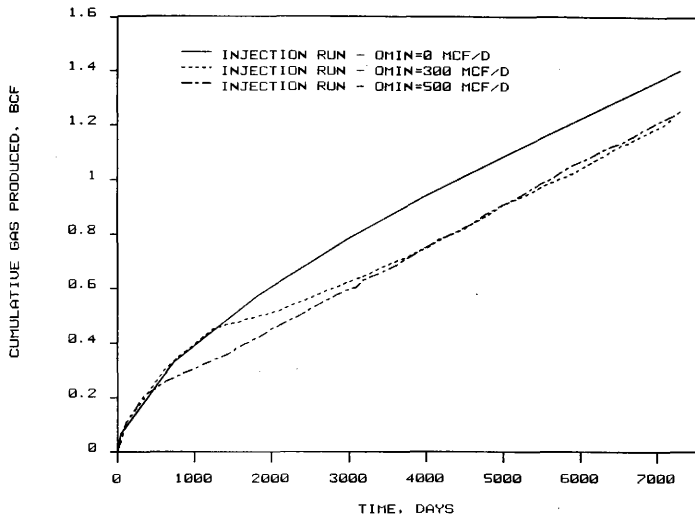


Fig. 36 - Effect of DMIN on Long Term Production using the Below Average Cotton Valley Lime Data Set for KR63, KR43, and PC6H1 Curves

no liquid loading problem. For example, to produce 1 Bcf of gas it would take 4440 days if the water could be efficiently removed from the wellbore. However, due to the liquid loading problem, it took 5700 days to produce 1 Bcf of gas. This is a difference of 3.45 years to produce the same amount of gas. This indicates that the critical gas flow rate,  $Q_{MIN}$ , can severely curtail long term production.

The sensitivity study of several parameters that was discussed previously in this thesis was conducted without considering the effect of the critical gas flow rate,  $Q_{MIN}$ . This means that during the sensitivity study, all the water that reached the wellbore was continuously removed, regardless of the gas flow rate. Therefore, the computer runs which were conducted during the sensitivity study represent ideal cases where all the water entering the wellbore was removed and no liquid loading occurred. In reviewing the results from the sensitivity study, the effects of relative permeability to gas and water on long term production were shown to be insignificant, as shown in Figures 18 and 14, respectively. However, this does not infer that the results will be the same when the critical gas flow rate is included.

The effect of relative permeability to water was investigated to determine if the same effect would occur when the critical gas flow rate,  $Q_{MIN}$ , was included. This was done using the two relative permeability to water curves in which the fracture fluid was mobile, the KRW2 and KRW3. The below average Cotton Valley Lime data set was used to investigate the effect of relative permeability to water using

a QMIN of 500 Mcf/D. Figure 37 illustrates the effect of relative permeability to water on long term production when using QMIN. It shows that QMIN does have an effect on long term production. However, the effect of relative permeability to water again has no effect on long term production. This indicates that the results from the sensitivity study are still useful. The only difference is that the results from the sensitivity study will be offset by a time increment. This time increment is due to the effect of the critical gas flow rate, QMIN. The time increment in Figure 37 is approximately 1250 days or 3.42 years.

To support this statement, the effect of formation damage was investigated in which the critical gas flow rate, QMIN was included. The below average data set and a QMIN of 500 Mcf/D were used in this part of the investigation. This run was compared to the cases where QMIN was not used, i.e. when QMIN is equal to 0 Mcf/D. Figure 38 presents the effect of formation damage on long term production when using QMIN. Because of the frequent liquid loading, the production history for the run which included QMIN is only shown for the first 3500 days. However, it is seen that when QMIN is included, the curve is shifted to the right, and therefore it takes longer to produce the same amount of gas. For example, to produce 0.4 Bcf of gas, it would take 1325 days if there was no damage. If the saturated region had a lower formation permeability of 50 percent due to formation damage, the 0.4 Bcf of gas would be produced in 1450 days. The difference between the ideal case and when there is formation damage is 125 days. However, when the effect of QMIN is included, it takes 2275 days to produce the

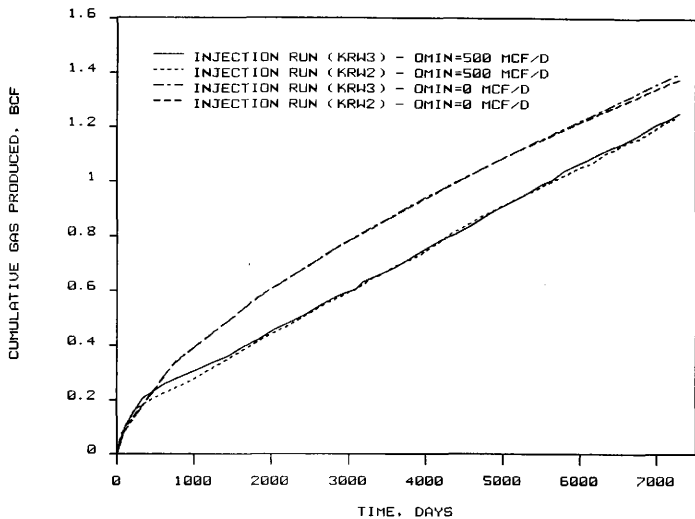


Fig. 37 - Effect of Relative Permeability to Water using the Below Average Cotton Valley Lime Data Set and OMIN for KR43 and PC441 Curves



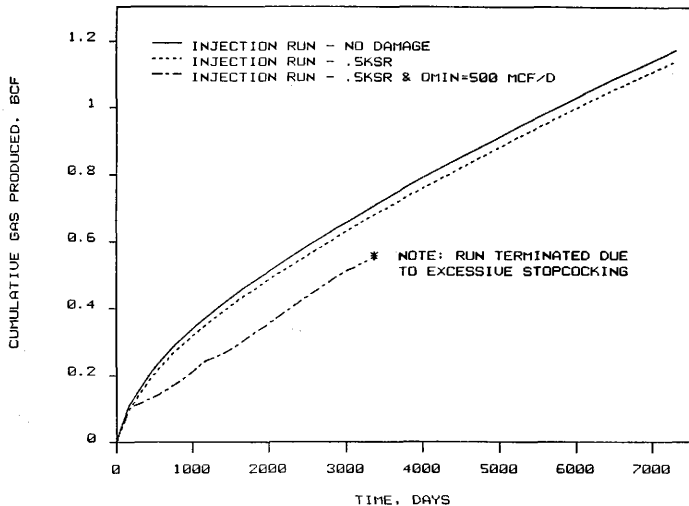


Fig. 38 - Effect of Formation Damage on Long Term Production using the Below Average Cotton Valley Lime Data Set & DMIN for KR61, KRH1, and PC6H1 Curves

same amount of gas. This adds another 825 days or 2.25 years to the time in which to produce the 0.4 Bcf of gas.

Since QMIN has a large effect on long term production, the question arose as to what could be done to minimize or eliminate the liquid loading problem. One answer is a very efficient method of removing the water from the wellbore, and there is always the possibility of restimulation. But restimulation can be expensive and lead to the same problem which already exists, and this study centers around the reservoir aspects of the problem. Therefore, one possible solution is the injection of an alcohol-methanol treatment to reduce the capillary pressure and change the relative permeability in the saturated region. However, it has already been shown that the effects of relative permeability to gas and water have very little effect on long term production. Figure 39 shows the effect of capillary pressure and QMIN on long term production for the below average Cotton Valley Lime data set. When QMIN is not included, there is a difference of approximately 200 days to produce 1 Bcf of gas. Therefore, a run was made in which capillary pressure in the saturated region was reduced. This run was made using the below average Cotton Valley Lime data set and a QMIN of 500 Mcf/D. The capillary pressure in the saturated region was reduced after the well loaded up with liquids for the first time. Figure 40 shows the effect of reducing the capillary pressure in the saturated region by 50 percent. There is an increase in production initially; however, there is no change in long term production. Therefore, it can be concluded that the best method of increasing gas production is to

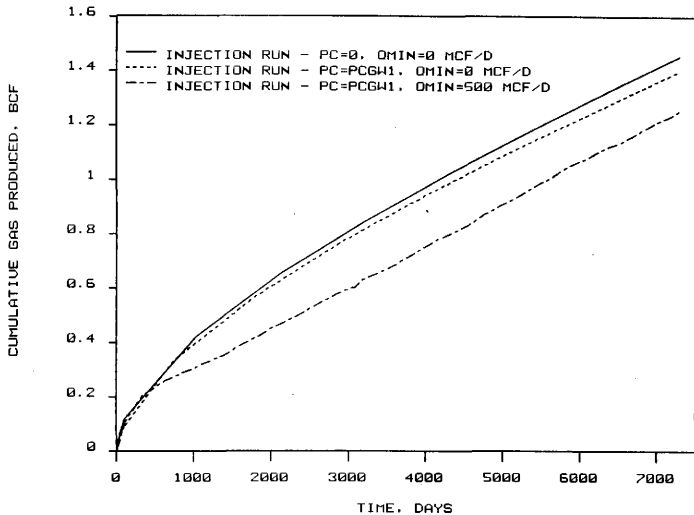


Fig. 39 - Effect of Capillary Pressure on Long Term Production using the Below Average Cotton Valley Lime Data Set and OMIN for KR63, KR43, and PCGW1 Curves

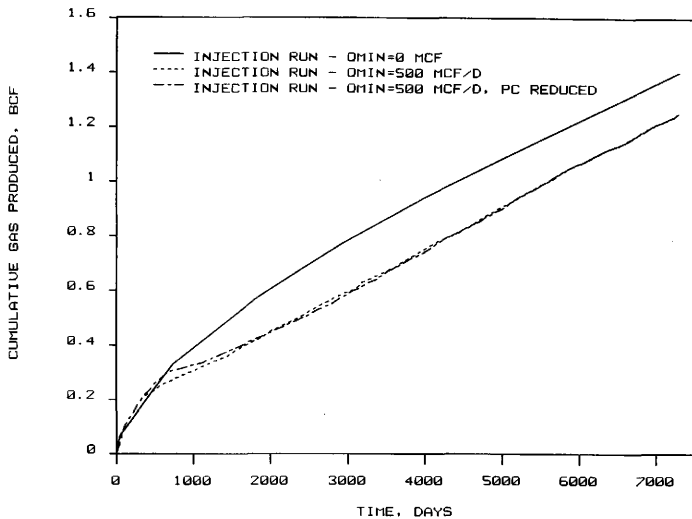


Fig. 40 - Effect of Reducing Capillary Pressure on Long Term Production using the Below Average Cotton Valley Lime Data Set and OMIN for KR63, KR43, and PCGH1 Curves

have an efficient method of removing the liquid from the wellbore.

## CONCLUSIONS

The following conclusions can be drawn from this study of liquid loading problems in hydraulically fractured gas wells. These conclusions are based on the capillary pressure and relative permeability curves presented in this thesis when using the average Cotton Valley Lime data sets.

1. For the reservoir properties simulated in this research, the presence of a high liquid saturated zone caused by the imbibition of fracture fluid around the fracture has very little effect on long term production when the liquid in the wellbore is continuously removed.
2. The liquid loading, which occurs in the gas wells simulated in this research, is caused by the fracture filling up with liquids. The fracture is merely an extension of the wellbore and fills up with liquid because the liquid is not efficiently removed from the wellbore.
3. Long term production can be significantly reduced due to the fracture loading up with liquids if the liquids are not efficiently removed from the wellbore.
4. The cleanup period following a hydraulic fracture treatment can last several weeks before gas production begins. This occurs when the irreducible gas saturation is greater than 30 percent and the fracture fluid remains immobile next to the fracture.

This emphasizes the importance of a thorough pre-fracture analysis before fracturing so that the well will not be prematurely abandoned.

5. Long term production was not affected by gas permeability hysteresis when the fracture fluid is mobile in the reservoir. However, if the fracture fluid is immobile, long term production will decline as the degree of gas permeability hysteresis increases.
6. When the fracture fluid is mobile in the reservoir, an increase in relative permeability to water only affects how fast the liquid in the saturated region is produced, and has no effect on long term production.
7. Long term production is reduced when the fracture fluid is immobile in the reservoir and remains essentially next to the fracture.
8. The relative permeability to gas had no effect on long term production when the relative permeability to gas curves are normalized to a gas relative permeability of 1 at the initial water saturation of 40 percent.
9. Long term production will be reduced by five percent when the effect of capillary pressure is included. However, the five percent reduction in long term production was not affected by the magnitude of capillary pressure used in this study.

10. The effect of formation damage on long term production becomes significant when the formation permeability in the saturated region is reduced by an order of magnitude or more.
11. As illustrated in Figure 36, the numerical value of QMIN, the critical gas flow rate, has little effect on long term production.
12. Reducing the capillary pressure around the fracture will only increase production in the short term. It will have no effect on long term production.
13. The computer model GASWAT can be used to model the liquid loading which occurs in these Cotton Valley Lime gas wells. This is illustrated in Figure 34 for the history-match of production data for the Prichard No. 1 well when using a QMIN of 300 Mcf/D. Also, the model has to be shut-in to allow the pressure to buildup in order to remove the liquid from the wellbore. This sequence of shutting the well in to allow the pressure to buildup is exactly what is being done in the field.
14. The following reservoir properties represent average values for the twenty Cotton Valley Lime wells analyzed in this study:

formation permeability = 0.004 md

total porosity = 6 percent

average water saturation = 20.5 percent

However, to model water production from the Cotton Valley Lime wells using a two-dimensional, two-phase reservoir model, the average water saturation had to be increased to 40 percent to obtain the liquid-gas ratios which occur in the field. The



total porosity was increased to 7.95 percent, so that the gas-in-place remained unchanged.

## NOMENCLATURE

DSGHYS = Water saturation change required to reduce KRG from the normal value at SGHYS, to zero, %

H = Net pay, ft

K = Formation permeability, md

K' = Consistency index

KRG = Relative permeability to gas, fraction

KRW = Relative permeability to water, fraction

KSR = Permeability in the saturated region, md

LAMDA = Degree of gas permeability hysteresis

n' = Flow behavior index

RKHYS = Relative permeability to gas at SGHYS, fraction

SGR = Irreducible gas saturation, %

SGHYS = Gas saturation at which gas permeability hysteresis begins, %

SW = Water saturation, %

SWR = Irreducible water saturation, %

XF = Fracture half length, ft

$\overline{XF}$  = Effective propped fracture length, ft

## REFERENCES

1. Duggan, J. O.: "Estimating Flow Rate Required to Keep Gas Wells Unloaded," J. Pet. Tech. (Dec. 1961) 1173-1176.
2. Turner, R. G., Hubbard, M. G. and Dukler, A. E.: "Analysis and Prediction of Minimum Flow Rate for the Continuous Removal of Liquids from Gas Wells," J. Pet. Tech. (Nov. 1969) 1475-1482.
3. Ilobi M. I. and Ikoku, C. U.: "Minimum Gas Flow Rate for Continuous Liquid Removal in Gas Wells," paper SPE 10170 presented at the SPE 56th Annual Fall Technical Conference and Exhibition, San Antonio, Texas, October 5-7, 1981.
4. MacDonald, R. M.: "Fluid Loading in Low Permeability Gas Wells in the Cotton Valley Sands of East Texas," paper SPE 9855 presented at the SPE/DOE Low Permeability Symposium, Denver, Colorado, May 27-29, 1981.
5. Libson, T. N. and Henry, J. R.: "Case Histories: Identification of and Remedial Action for Liquid Loading in Gas Wells—Intermediate Shelf Gas Play," J. Pet. Tech. (April 1980) 685-693.
6. Henderson, L. J.: "Deep Sucker Rod Pumping for Gas Well Unloading," paper SPE 13199 presented at the SPE 59th Annual Technical Conference and Exhibition, Houston, Texas, Sept. 16-19, 1984.
7. Vosida, J. L.: "Use of Foaming Agents to Alleviate Liquid Loading in Greater Green River TFG Wells," paper SPE 11644 presented at the SPE/DOE Symposium on Low Permeability, Denver, Colorado, March 14-16, 1983.
8. Tannich, J. D.: "Liquid Removal from Hydraulically Fractured Gas Wells," J. Pet. Tech. (Nov. 1975) 1309-1317.
9. Holditch, S. A.: "Factors Affecting Water Blocking and Gas Flow From Hydraulically Fractured Gas Wells," J. Pet. Tech. (Dec. 1979) 1515-1524.
10. "Cotton Valley Limestone Study," Mitchell Energy Corp., Houston (Oct. 1984) Section V 1,14.
11. Horner, D.R.: "Pressure Buildup In Wells," Proc., Third World Pet. Cong., The Hague (1951), Sec. 2, 503-523; Reprint Series No. 9—Pressure Analysis Methods, Society of Petroleum Engineers of AIME, Dallas (1967) 25-43.

12. Gringarten, A.C., Bourdet, P.D., Landel, P.A., and Kniazeff, V.J.: "A Comparison Between Different Skin and Wellbore Storage Type-Curves for Early-Time Transient Analysis," paper SPE 8205 presented at the SPE 1979 Annual Fall Technical Conference and Exhibition, Las Vegas, September 23-26.
13. Cinco-Ley, H. and Samaniego F.V.: "Transient Pressure Analysis for Fractured Wells," J. Pet. Tech. (Sept. 1981) 1749-1766.
14. Killough, J.E.: "Reservoir Simulation with History - Dependent Saturation Functions," paper SPE 5106 presented at the 49th Annual Fall Meeting of the SPE in Houston, Texas, October 6-9, 1974.
15. Gertsma, J. and deKlerk F.: "A Rapid Method of Predicting Width and Extent of Hydraulically Induced Fractures," J. Pet. Tech. (Dec. 1969) 1571-1581.
16. Cooke, C.E.: "Conductivity of Fracture Proppants in Multiple Layers," J. Pet. Tech. (Sept. 1973) 1101-1107; Trans., AIME, 255.

## APPENDIX A

PROPTRAN is a computer model designed to calculate the proppant concentration in a vertical, hydraulic fracture. The created dimensions are computed using the equations of Gertsma and deKlerk.<sup>15</sup> The model uses the created dimensions to develop a grid pattern to model the proppant as it is transported down the fracture. Using the developed grid pattern, a finite difference numerical method technique calculates the movement of both the fluid and the proppant down the fracture as a function of time. The proppant settling is taken into account by using Stoke's law with provisions made for hindering settling velocity.

The input data needed for the computer model are listed in Table A-1. The output from the model is divided into two sections, the fracture dimension and proppant transport sections, respectively. The section on fracture dimension analysis is shown in Table A-2. It reports both the created and propped dimensions as well as the fracture conductivity as a function of fluid volume injected. In the proppant transport analysis section, the concentration of proppant down the fracture is shown in Table A-3. Knowing where the net pay is located within the fracture, the effective propped fracture length can be determined. Using the effective propped fracture length, the fracture conductivity is then determined from the fracture dimension section.

TABLE A-1  
INPUT DATA FOR COMPUTER MODEL PROPTRAN

WELL COMPLETION DATA

|                             |        |                                |        |
|-----------------------------|--------|--------------------------------|--------|
| FORMATION DEPTH (FT).....   | 10669. | PACKER DEPTH (FT).....         | 10550. |
| TUBING I.D. (IN).....       | 2.441  | TUBING O.D. (IN).....          | 2.875  |
| CASING I.D. (IN).....       | 4.892  | WELLBORE DIAMETER (IN).....    | 5.500  |
| NUMBER OF PERFORATIONS..... | 25     | PERFORATION DIAMETER (IN)..... | 0.340  |

FORMATION DATA

|                              |        |                                |             |
|------------------------------|--------|--------------------------------|-------------|
| FRAC GRAD. (PSI/FT).....     | 0.76   | RES. FLUID VISC. (CP).....     | 0.020       |
| POROSITY (%).....            | 5.7    | RES. FLUID COMP. (PSI-1)...    | 0.000163    |
| PERMEABILITY (MD).....       | 0.0010 | GROSS FRACTURE HEIGHT (FT).... | 247.        |
| WELL SPACING (ACRES).....    | 640.   | NET FRACTURE HEIGHT (FT).....  | 142.        |
| RESERVOIR PRESSURE (PSI).... | 6134.  | YOUNG'S MODULUS (PSI).....     | 0.10500E+08 |
| BOTTOMHOLE TEMP. (DEG F).... | 285.   | POISSON'S RATIO.....           | 0.300       |

FRAC FLUID AND PROPPANT DATA

|                               |        |                                |        |
|-------------------------------|--------|--------------------------------|--------|
| FRAC FLUID GRAD. (PSI/FT).... | 0.440  | N2-WATER RATIO (SCF/BBL).....  | 0.     |
| N'.....                       | 0.7000 | K' (LB/SEC**N'/SQFT).....      | 0.0047 |
| SPURT LOSS COEFF (GAL/SQFT).. | 0.0000 | CW - FLUID LOSS (FT/SQRTMIN).. | 0.0019 |
| PROPPANT DENSITY (GM/CC)..... | 2.650  | PROPPANT DIAMETER (IN).....    | 0.0273 |

PUMPING SCHEDULE

180000. GALLONS - PAD VOLUME  
 10000. GALLONS WITH 1.0 PPG OF 20/40 MESH SAND  
 10000. GALLONS WITH 2.0 PPG OF 20/40 MESH SAND  
 10000. GALLONS WITH 3.0 PPG OF 20/40 MESH SAND  
 50000. GALLONS WITH 4.0 PPG OF 20/40 MESH SAND  
 50000. GALLONS WITH 4.0 PPG OF 20/40 MESH SAND  
 90000. GALLONS WITH 5.0 PPG OF 20/40 MESH SAND  
 22890. GALLONS WITH 6.0 PPG OF 20/40 MESH SAND

TREATMENT PARAMETERS

|   |       |
|---|-------|
| RATE (BPM).....                         | 20.0  |
| SURFACE TREATING PRESSURE (PSI).....    | 8311. |
| PIPE FRICTION (PSI).....                | 4748. |
| PERFORATION FRICTION (PSI).....         | 106.  |
| BOTTOMHOLE TREATING PRESSURE (PSI)..... | 8151. |
| HORSEPOWER REQUIREMENTS (HHP).....      | 4072. |
| CLOSURE PRESSURE ON PROPPANT (PSI)..... | 6951. |

TABLE A-2  
 FRACTURE DIMENSION ANALYSIS  
 USING COMPUTER MODEL PROPTRAM

|                                   |         |         |         |         |         |
|-----------------------------------|---------|---------|---------|---------|---------|
| VOLUME (GALS)                     | 42289.  | 84578.  | 126867. | 169156. | 211445. |
| CREATED LENGTH (FT)               | 761.    | 1178.   | 1520.   | 1822.   | 2096.   |
| PROPPED LENGTH (FT)               | 401.    | 620.    | 801.    | 960.    | 1105.   |
| CREATED WIDTH (IN)                | 0.192   | 0.248   | 0.289   | 0.321   | 0.349   |
| PROPPED WIDTH (IN)                | 0.055   | 0.071   | 0.082   | 0.092   | 0.100   |
| PROPPED HEIGHT (FT)               | 247.    | 247.    | 247.    | 247.    | 247.    |
| APPARENT VISC. (CP)               | 59.     | 68.     | 75.     | 90.     | 94.     |
| PROD. INCREASE                    | 4.37    | 5.64    | 6.75    | 7.74    | 6.97    |
| FRAC COND. (MD-FT)                | 196.    | 253.    | 294.    | 327.    | 355.    |
| DIMEN. FRAC COND.                 | 155.3   | 129.8   | 116.8   | 108.4   | 102.3   |
| PROP CONC. (LBS/FT <sup>2</sup> ) | 0.53    | 0.68    | 0.79    | 0.88    | 0.96    |
| TOTAL PROPPANT (LBS)              | 104734. | 209468. | 314202. | 418936. | 523670. |

|                                   |         |         |         |         |          |
|-----------------------------------|---------|---------|---------|---------|----------|
| VOLUME (GALS)                     | 253734. | 296023. | 338312. | 380601. | 422890.  |
| CREATED LENGTH (FT)               | 2351.   | 2590.   | 2817.   | 3034.   | 3242.    |
| PROPPED LENGTH (FT)               | 1240.   | 1366.   | 1486.   | 1600.   | 1710.    |
| CREATED WIDTH (IN)                | 0.373   | 0.395   | 0.415   | 0.433   | 0.451    |
| PROPPED WIDTH (IN)                | 0.107   | 0.113   | 0.119   | 0.124   | 0.129    |
| PROPPED HEIGHT (FT)               | 247.    | 247.    | 247.    | 247.    | 247.     |
| APPARENT VISC. (CP)               | 87.     | 90.     | 93.     | 95.     | 98.      |
| PROD. INCREASE                    | 7.46    | 8.24    | 8.98    | 9.28    | 9.82     |
| FRAC COND. (MD-FT)                | 380.    | 402.    | 423.    | 441.    | 459.     |
| DIMEN. FRAC COND.                 | 97.5    | 93.7    | 90.5    | 87.8    | 85.4     |
| PROP CONC. (LBS/FT <sup>2</sup> ) | 1.03    | 1.09    | 1.14    | 1.19    | 1.24     |
| TOTAL PROPPANT (LBS)              | 628404. | 733138. | 837872. | 942606. | 1047340. |





## APPENDIX B

TYPEFIN is a computer model designed to forecast well performance of a gas or oil reservoir containing a finite conductivity, vertical hydraulic fracture. The model predicts reservoir performance by utilizing solutions generated using a finite difference model to solve the fluid flow equation for the specified formation and fracture parameters. The model is not exact however due to its simplifying assumptions made in the development of the type-curve solutions. The two critical assumptions for the gas well solution are a fluid of constant viscosity and that the fluid compressibility is small and constant. However, by using real-gas pseudopressure and pseudotime, the error associated with these assumptions is greatly reduced.

Table B-1 represents the input data needed to run the model TYPEFIN. The fracture length and fracture conductivity are determined from the previous model PROPTRAN. The well's forecasted performance is shown in Table B-2.

TABLE B-1  
INPUT DATA FOR COMPUTER MODEL TYPEFIN

OPERATOR: MITCHELL ENERGY CORP.  
WELL: PRICHARD NO. 1  
LOCATION: LIMESTONE, COUNTY  
FORMATION: COTTEN VALLEY LIME

|                                     |             |             |
|-------------------------------------|-------------|-------------|
| GAS GRAVITY                         | (AIR=1)     | 0.60000     |
| BOTTOM HOLE TEMPERATURE             | - DEGREES F | 285.00000   |
| MOLE PERCENT H2S                    | - PERCENT   | 0.00000     |
| MOLE PERCENT CO2                    | - PERCENT   | 0.00000     |
| MOLE PERCENT N2                     | - PERCENT   | 0.00000     |
| INITIAL RESERVOIR PRESSURE          | - PSIA      | 6134.00000  |
| FORMATION PERMEABILITY              | - MD        | 0.00100     |
| FORMATION POROSITY                  | - FRACTION  | 0.05700     |
| WATER SATURATION                    | - FRACTION  | 0.12700     |
| WATER COMPRESSIBILITY               | - PSI-1     | 0.0000035   |
| FORMATION COMPRESSIBILITY           | - PSI-1     | 0.0000040   |
| FORMATION NET GAS PAY               | - FEET      | 49.00000    |
| FRACTURE LENGTH                     | - FEET      | 1254.00000  |
| FRACTURE CONDUCTIVITY               | - MD-FT     | 529.00000   |
| DIMENSIONLESS FRACTURE CONDUCTIVITY |             | 248.66511   |
| DRAINAGE ACREAGE                    | - ACRES     | 640.00000   |
| ORIGINAL GAS IN PLACE               | - MCF       | 0.17747E+08 |
| ECONOMIC LIMIT                      | - MCFD      | 1.00000     |
| DIMENSIONLESS FRACTURE PENETRATION  |             | 2.10532     |

CONSTANT PRESSURE SCHEDULE

| INTERVAL | LENGTH OF<br>INTERVAL<br>(DAYS) | TIME STEP<br>SIZE<br>(DAYS) | WELL BORE<br>PRESSURE<br>(PSIA) |
|----------|---------------------------------|-----------------------------|---------------------------------|
| 1        | 1630.                           | 40.00                       | 850.0                           |

TABLE B-2  
WELL PERFORMANCE PREDICTED BY COMPUTER MODEL TYPEFIN

| TIME<br>(DAYS) | CUM GAS<br>PRODUCED<br>(MCF) | CUM GAS<br>PRODUCED<br>(%OGIP) | AVERAGE<br>PRESSURE<br>(PSIA) | AVERAGE<br>FLOW RATE<br>(MCF/D) | WELL BORE<br>PRESSURE<br>(PSIA) |
|----------------|------------------------------|--------------------------------|-------------------------------|---------------------------------|---------------------------------|
| 40.00          | 0.5779E+05                   | 0.3256                         | 6104.                         | 1445.                           | 850.0                           |
| 80.00          | 0.8418E+05                   | 0.4744                         | 6091.                         | 659.9                           | 850.0                           |
| 120.0          | 0.1046E+06                   | 0.5894                         | 6080.                         | 510.5                           | 850.0                           |
| 160.0          | 0.1219E+06                   | 0.6871                         | 6071.                         | 433.3                           | 850.0                           |
| 200.0          | 0.1373E+06                   | 0.7737                         | 6063.                         | 384.1                           | 850.0                           |
| 240.0          | 0.1513E+06                   | 0.8524                         | 6056.                         | 349.3                           | 850.0                           |
| 280.0          | 0.1642E+06                   | 0.9252                         | 6049.                         | 322.9                           | 850.0                           |
| 320.0          | 0.1763E+06                   | 0.9932                         | 6043.                         | 302.0                           | 850.0                           |
| 360.0          | 0.1877E+06                   | 1.057                          | 6037.                         | 284.9                           | 850.0                           |
| 400.0          | 0.1985E+06                   | 1.118                          | 6032.                         | 270.6                           | 850.0                           |
| 440.0          | 0.2088E+06                   | 1.177                          | 6026.                         | 258.4                           | 850.0                           |
| 480.0          | 0.2187E+06                   | 1.233                          | 6021.                         | 247.8                           | 850.0                           |
| 520.0          | 0.2283E+06                   | 1.286                          | 6016.                         | 238.5                           | 850.0                           |
| 560.0          | 0.2375E+06                   | 1.338                          | 6012.                         | 230.3                           | 850.0                           |
| 600.0          | 0.2464E+06                   | 1.388                          | 6007.                         | 222.9                           | 850.0                           |
| 640.0          | 0.2551E+06                   | 1.437                          | 6003.                         | 216.3                           | 850.0                           |
| 680.0          | 0.2635E+06                   | 1.485                          | 5998.                         | 210.2                           | 850.0                           |
| 720.0          | 0.2717E+06                   | 1.531                          | 5994.                         | 204.7                           | 850.0                           |
| 760.0          | 0.2796E+06                   | 1.576                          | 5990.                         | 199.7                           | 850.0                           |
| 800.0          | 0.2874E+06                   | 1.620                          | 5986.                         | 195.0                           | 850.0                           |
| 840.0          | 0.2951E+06                   | 1.663                          | 5982.                         | 190.7                           | 850.0                           |
| 880.0          | 0.3025E+06                   | 1.705                          | 5979.                         | 186.7                           | 850.0                           |
| 920.0          | 0.3099E+06                   | 1.746                          | 5975.                         | 182.9                           | 850.0                           |
| 960.0          | 0.3170E+06                   | 1.786                          | 5971.                         | 179.4                           | 850.0                           |
| 1000.          | 0.3241E+06                   | 1.826                          | 5968.                         | 176.1                           | 850.0                           |
| 1040.          | 0.3310E+06                   | 1.865                          | 5964.                         | 173.0                           | 850.0                           |
| 1080.          | 0.3378E+06                   | 1.903                          | 5961.                         | 170.1                           | 850.0                           |
| 1120.          | 0.3445E+06                   | 1.941                          | 5957.                         | 167.4                           | 850.0                           |
| 1160.          | 0.3511E+06                   | 1.978                          | 5954.                         | 164.7                           | 850.0                           |
| 1200.          | 0.3576E+06                   | 2.015                          | 5951.                         | 162.3                           | 850.0                           |
| 1240.          | 0.3640E+06                   | 2.051                          | 5948.                         | 159.9                           | 850.0                           |
| 1280.          | 0.3703E+06                   | 2.086                          | 5944.                         | 157.7                           | 850.0                           |
| 1320.          | 0.3765E+06                   | 2.122                          | 5941.                         | 155.5                           | 850.0                           |
| 1360.          | 0.3826E+06                   | 2.156                          | 5938.                         | 153.5                           | 850.0                           |
| 1400.          | 0.3887E+06                   | 2.190                          | 5935.                         | 151.5                           | 850.0                           |
| 1440.          | 0.3947E+06                   | 2.224                          | 5932.                         | 149.6                           | 850.0                           |
| 1480.          | 0.4006E+06                   | 2.257                          | 5929.                         | 147.8                           | 850.0                           |
| 1520.          | 0.4064E+06                   | 2.290                          | 5926.                         | 146.1                           | 850.0                           |
| 1560.          | 0.4122E+06                   | 2.323                          | 5923.                         | 144.4                           | 850.0                           |
| 1600.          | 0.4179E+06                   | 2.355                          | 5920.                         | 142.8                           | 850.0                           |
| 1630.          | 0.4222E+06                   | 2.379                          | 5918.                         | 141.5                           | 850.0                           |

## APPENDIX C

FRACSIM is a computer model designed specifically to forecast the production of a vertically fractured gas well. However, it can also be used to model the performance of an oil well. The model is a single-phase, two-dimensional model used to simulate the flow of a single phase fluid in porous media. FRACSIM is equipped to handle such factors as reservoir heterogeneity and formation damage. And the effects of non-Darcy flow and fracture closure can also be included into the model as well as the effects of formation permeability reduction. The fracture length, fracture width, and drainage area are all controlled by the grid dimensions which are input into the model. Table C-1 lists some of the grid patterns used for different fracture lengths and drainage areas.

The input data used to run the model FRACSIM are listed in Table C-2. Included in the input data are control keys to include the non-Darcy flow, fracture closure, and permeability reduction effects. The constants A and B in Cooke's equation<sup>16</sup> depend on the proppant used to prop the fracture open and are needed to calculate the non-Darcy flow effects. Table C-3 shows the permeability reduction due to fracture closure for 20/40 mesh sand which is also part of the input data. The output from FRACSIM is composed of two parts: (1) the actual time steps and (2) a summary table. At each time step, the pressure at each grid block, the flow rate, cumulative gas produced, and average reservoir pressure are printed as illustrated by Table C-4. A composite summary of each time step is shown in Table C-5.

TABLE C-1  
GRID PATTERNS USED FOR COMPUTER MODEL FRACSIM

DRAINAGE AREA = 640 ACRES

| Fracture Length (ft) | <u>Length of Cells in x-direction (ft)</u>  |
|----------------------|---|
| 500                  | 0.001, 5, 15, 45, 120, 130, 120, 45, 15, 5, 5, 15, 45, 135, 485, 485, 485, 485      |
| 1000                 | 0.001, 5, 15, 45, 135, 200, 200, 200, 135, 45, 15, 5, 5, 15, 45, 135, 480, 480, 480 |
| 1500                 | 0.001, 5, 15, 45, 135, 275, 275, 275, 275, 135, 45, 15, 5, 5, 15, 45, 135, 470, 470 |
| 2000                 | 0.001, 5, 15, 45, 135, 320, 320, 320, 320, 135, 45, 15, 5, 5, 15, 45, 135, 440      |
|                      | <u>Length of Cells in y-direction (ft)</u>  |
|                      | 0.004, 0.5, 1.5, 4.5, 13.5, 40.5, 121.5, 400, 400, 400, 400, 400, 458               |

DRAINAGE AREA = 320 ACRES

| Fracture Length (ft) | <u>Length of Cells in x-direction (ft)</u>                                     |
|----------------------|--|
| 1000                 | 0.001, 5, 15, 45, 135, 200, 200, 200, 135, 45, 15, 5, 5, 15, 45, 135, 330, 337 |
| 1500                 | 0.001, 5, 15, 45, 135, 275, 275, 275, 275, 135, 45, 15, 5, 5, 15, 45, 150, 152 |
|                      | <u>Length of Cells in y-direction (ft)</u>                                     |
|                      | 0.004, 0.5, 1.5, 4.5, 13.5, 40.5, 121.5, 280, 280, 280, 280, 280, 285          |

TABLE C-2  
INPUT DATA FOR COMPUTER MODEL FRACSIM

## RESERVOIR DATA

|                        |             |        |
|------------------------|-------------|--------|
| ORIGINAL PRESSURE      | - PSI       | 6134.  |
| DEPTH OF FORMATION     | - FEET      | 10675. |
| FORMATION PERMEABILITY | - MD        | 0.0012 |
| GAS POROSITY           | - FRACTION  | 0.050  |
| NET PAY                | - FEET      | 49.0   |
| FRACTURE PERMEABILITY  | - MD        | 3.5E05 |
| FRACTURE POROSITY      | - FRACTION  | 0.200  |
| FRACTURE LENGTH        | - FEET      | 900.0  |
| FRACTURE HEIGHT        | - FEET      | 247.0  |
| FRACTURE GRADIENT      | - PSI/FEET  | 0.764  |
| BOTTOMHOLE TEMPERATURE | - DEGREES F | 285.0  |
| GAS GRAVITY            | (AIR=1)     | 0.600  |
| DRAINAGE AREA          | - ACRES     | 640    |

## WELL CONTROL DATA

|   |            |       |
|---|------------|-------|
| NON-DARCY FLOW EFFECTS                              |            | YES   |
| FRACTURE CLOSURE AND PERMEABILITY REDUCTION EFFECTS |            | YES   |
| CONSTANT 'A' IN COOKE'S EQN.                        |            | 1.54  |
| CONSTANT 'B' IN COOKE'S EQN.                        |            | 2.65  |
| CONVERGENCE CRITERIA                                | - PSI      | 1.0   |
| MAXIMUM GAS PRODUCED PER STEP                       | - % OF GIP | 5.0   |
| MAXIMUM PRESSURE DROP PER STEP IN ANY CELL          | - PSI      | 2000. |

## CONSTANT PRESSURE SCHEDULE

| INTERVAL | LENGTH OF<br>INTERVAL<br>(DAYS) | TIME STEP<br>SIZE<br>(DAYS) | BOTTOMHOLE<br>PRESSURE<br>(PSIA) |
|----------|---------------------------------|-----------------------------|----------------------------------|
| 1        | 1630.                           | 50.00                       | 1039.0                           |

TABLE C-3  
FRACTURE CLOSURE FOR 20/40 MESH SAND

| <u>CLOSURE<br/>PRESSURE</u> | <u>FRACTION OF ORIGINAL<br/>PERMEABILITY</u> |
|-----------------------------|--|
| 0.0                         | 1.0  |
| 1000.0                      | 0.900  |
| 2000.0                      | 0.783  |
| 3000.0                      | 0.650  |
| 4000.0                      | 0.500  |
| 5000.0                      | 0.340  |
| 6000.0                      | 0.233  |
| 7000.0                      | 0.147  |
| 8000.0                      | 0.100  |
| 9000.0                      | 0.070  |
| 10000.0                     | 0.050  |
| 11000.0                     | 0.040  |

TABLE C-4  
TIME STEP FROM COMPUTER MODEL FRACTSIN

| STEP= 10   | TIME= 361.00                            | DELTA= 90.000 |                                   |           |           |           |           |           |           |           |           | CYCLES= 38                               |
|--|---|---------------|-----------------------------------|-----------|-----------|-----------|-----------|-----------|-----------|-----------|-----------|--|
| FLOW RATE= 890.38 MCF/D                                    | AVERAGE RESERVOIR PRESSURE= 8053.1 PSI  |               |                                   |           |           |           |           |           |           |           |           | CUMULATIVE GAS PRODUCED= 0.189316 06 MCF |
| PERCENT GAS PRODUCED= 1.0618                               | REMAINING GAS IN PLACE= 0.178416 08 MCF |               |                                   |           |           |           |           |           |           |           |           | PERCENT ERROR= 0.55497E-05               |
| WELL PRODUCTIVITY INDEX= 0.14680E-09 REC MCF/CP/DAY/PSI**2 |   |               |                                   |           |           |           |           |           |           |           |           |  |
| ACTUAL FRACTURE CONDUCTIVITY, MD-FT                        |   |               |                                   |           |           |           |           |           |           |           |           |  |
| 396.242  | 396.422                                 | 397.134       | 399.182                           | 404.643   | 411.710   | 421.678   | 428.089   | 431.361   | 432.255   | 432.402   | 432.424   |  |
| EFFECTIVE FRACTURE CONDUCTIVITY, MD-FT                     |   |               |                                   |           |           |           |           |           |           |           |           |  |
| 269.370  | 269.752                                 | 271.268       | 275.769                           | 289.082   | 311.054   | 339.708   | 368.270   | 395.098   | 413.661   | 422.991   | 429.411   |  |
| NON-DARCY FACTORS IN X-DIRECTION                           |   |               |                                   |           |           |           |           |           |           |           |           |  |
| 0.67981  | 0.68047                                 | 0.68306       | 0.69083                           | 0.71441   | 0.75552   | 0.80561   | 0.86027   | 0.91593   | 0.95699   | 0.97824   | 0.99303   |  |
| X-DIRECTION PERMEABILITIES - MD                            |   |               |                                   |           |           |           |           |           |           |           |           |  |
| 0.4950 05  | 0.4950 05                               | 0.4950 05     | 0.4990 05                         | 0.4990 05 | 0.5060 05 | 0.5150 05 | 0.5270 05 | 0.5350 05 | 0.5390 05 | 0.5400 05 | 0.5410 05 | 0.5410 06                                |
| Y-DIRECTION PERMEABILITIES - MD                            |   |               |                                   |           |           |           |           |           |           |           |           |  |
| 0.3500 06  | 0.3500 06                               | 0.3500 06     | 0.3500 06                         | 0.3500 06 | 0.3500 06 | 0.3500 06 | 0.3500 06 | 0.3500 06 | 0.3500 06 | 0.3500 06 | 0.3500 06 | 0.3500 06                                |
| FWFD= 0.37908  | TD= 0.28697E-01                         | GR= 96.956    | AVERAGE FRAC CONDUCTIVITY= 335.76 |           |           |           |           |           |           |           |           |  |
| CALCULATED PRESSURES                                       |   |               |                                   |           |           |           |           |           |           |           |           |  |
| 1059.391   | 1054.415                                | 1059.073      | 1072.854                          | 1110.070  | 1158.875  | 1196.808  | 1221.811  | 1235.518  | 1244.052  | 1257.414  | 1304.375  |  |
| 1109.335   | 1109.336                                | 1113.268      | 1126.068                          | 1161.447  | 1207.991  | 1244.849  | 1269.355  | 1285.711  | 1312.904  | 1374.160  | 1555.410  |  |
| 1259.956   | 1259.957                                | 1262.409      | 1272.897                          | 1304.004  | 1345.963  | 1379.572  | 1402.990  | 1426.510  | 1502.168  | 1876.563  | 2024.712  |  |
| 1833.711   | 1833.711                                | 1834.538      | 1846.946                          | 1864.543  | 1898.802  | 1726.375  | 1748.294  | 1789.019  | 1971.303  | 2324.836  | 2652.438  |  |
| 2452.745   | 2452.745                                | 2452.945      | 2455.194                          | 2469.118  | 2493.122  | 2514.096  | 2536.099  | 2511.978  | 2957.733  | 3327.316  | 3493.340  |  |
| 4038.530   | 4036.530                                | 4036.577      | 4037.116                          | 4042.121  | 4055.565  | 4069.824  | 4096.021  | 4211.828  | 4518.926  | 4676.112  | 4733.270  |  |
| 5897.548   | 5897.548                                | 5897.652      | 5897.700                          | 5898.157  | 5899.944  | 5902.754  | 5909.832  | 5932.707  | 5967.787  | 5981.606  | 5986.290  |  |
| 6120.405   | 6120.405                                | 6120.405      | 6120.408                          | 6120.435  | 6120.556  | 6120.786  | 6121.379  | 6122.978  | 6124.918  | 6125.633  | 6125.877  |  |
| 6133.368   | 6133.368                                | 6133.368      | 6133.368                          | 6133.370  | 6133.376  | 6133.390  | 6133.424  | 6133.505  | 6133.590  | 6133.621  | 6133.631  |  |
| 6133.975   | 6133.975                                | 6133.975      | 6133.975                          | 6133.975  | 6133.975  | 6133.976  | 6133.977  | 6133.981  | 6133.984  | 6133.985  | 6133.985  |  |
| 6133.999   | 6133.999                                | 6133.999      | 6133.999                          | 6133.999  | 6133.999  | 6133.999  | 6133.999  | 6133.999  | 6133.999  | 6133.999  | 6133.999  |  |
| 6134.000   | 6134.000                                | 6134.000      | 6134.000                          | 6134.000  | 6134.000  | 6134.000  | 6134.000  | 6134.000  | 6134.000  | 6134.000  | 6134.000  |  |
| 2400.265   | 3147.743                                | 4130.677      | 5329.858                          | 6091.348  | 6132.779  | 6133.970  |           |           |           |           |           |  |
| 2400.324   | 3147.745                                | 4130.677      | 5329.858                          | 6091.348  | 6132.779  | 6133.970  |           |           |           |           |           |  |
| 2410.093   | 3148.945                                | 4130.844      | 5329.860                          | 6091.349  | 6132.779  | 6133.970  |           |           |           |           |           |  |
| 2456.701   | 3161.747                                | 4132.826      | 5329.142                          | 6091.356  | 6132.779  | 6133.970  |           |           |           |           |           |  |
| 2856.778   | 3270.448                                | 4151.843      | 5332.688                          | 6091.429  | 6132.780  | 6133.970  |           |           |           |           |           |  |
| 3581.148   | 3762.856                                | 4306.089      | 5355.713                          | 6092.094  | 6132.795  | 6133.970  |           |           |           |           |           |  |
| 4762.493   | 4822.084                                | 5007.247      | 5532.731                          | 6097.780  | 6132.920  | 6133.973  |           |           |           |           |           |  |
| 5988.808   | 5993.689                                | 6008.668      | 6053.747                          | 6127.782  | 6133.779  | 6133.994  |           |           |           |           |           |  |
| 6125.999   | 6126.245                                | 6126.989      | 6129.187                          | 6133.558  | 6133.982  | 6133.999  |           |           |           |           |           |  |
| 6133.536   | 6133.647                                | 6133.678      | 6133.770                          | 6133.976  | 6133.999  | 6134.000  |           |           |           |           |           |  |
| 6133.986   | 6133.986                                | 6133.987      | 6133.991                          | 6133.999  | 6134.000  | 6134.000  |           |           |           |           |           |  |
| 6133.999   | 6133.999                                | 6134.000      | 6134.000                          | 6134.000  | 6134.000  | 6134.000  |           |           |           |           |           |  |
| 6134.000   | 6134.000                                | 6134.000      | 6134.000                          | 6134.000  | 6134.000  | 6134.000  |           |           |           |           |           |  |



TABLE C-5  
SUMMARY TABLE FROM COMPUTER MODEL FRACSIM

| TIME<br>DAYS | FLOW<br>RATE<br>MCFD | CUMULATIVE<br>PRODUCTION<br>MCF | RECOVERY<br>EFFICIENCY<br>% OGIP | FLOWING<br>BOTTOM HOLE<br>PRESSURE<br>PSI | AVERAGE<br>RESERVOIR<br>PRESSURE<br>PSI |
|--------------|----------------------|---------------------------------|----------------------------------|---|---|
| 1.000        | 9101.                | 9101.                           | 0.5104E-01                       | 1039.                                     | 6130.                                   |
| 6.000        | 1898.                | 0.1859E 05                      | 0.1043                           | 1039.                                     | 6126.                                   |
| 31.00        | 1092.                | 0.4588E 05                      | 0.2573                           | 1039.                                     | 6114.                                   |
| 81.00        | 671.0                | 0.7944E 05                      | 0.4455                           | 1039.                                     | 6100.                                   |
| 131.0        | 503.7                | 0.1046E 06                      | 0.5868                           | 1039.                                     | 6089.                                   |
| 181.0        | 417.8                | 0.1255E 06                      | 0.7039                           | 1039.                                     | 6080.                                   |
| 231.0        | 365.2                | 0.1438E 06                      | 0.8063                           | 1039.                                     | 6072.                                   |
| 281.0        | 328.8                | 0.1602E 06                      | 0.8985                           | 1039.                                     | 6065.                                   |
| 331.0        | 301.7                | 0.1753E 06                      | 0.9831                           | 1039.                                     | 6059.                                   |
| 381.0        | 280.4                | 0.1893E 06                      | 1.062                            | 1039.                                     | 6053.                                   |
| 431.0        | 263.1                | 0.2025E 06                      | 1.136                            | 1039.                                     | 6048.                                   |
| 481.0        | 248.7                | 0.2149E 06                      | 1.205                            | 1039.                                     | 6042.                                   |
| 531.0        | 236.4                | 0.2267E 06                      | 1.272                            | 1039.                                     | 6037.                                   |
| 581.0        | 225.9                | 0.2380E 06                      | 1.335                            | 1039.                                     | 6032.                                   |
| 631.0        | 216.8                | 0.2489E 06                      | 1.396                            | 1039.                                     | 6028.                                   |
| 681.0        | 208.9                | 0.2593E 06                      | 1.454                            | 1039.                                     | 6023.                                   |
| 731.0        | 201.9                | 0.2694E 06                      | 1.511                            | 1039.                                     | 6019.                                   |
| 781.0        | 195.7                | 0.2792E 06                      | 1.566                            | 1039.                                     | 6014.                                   |
| 831.0        | 190.2                | 0.2887E 06                      | 1.619                            | 1039.                                     | 6010.                                   |
| 881.0        | 185.2                | 0.2980E 06                      | 1.671                            | 1039.                                     | 6006.                                   |
| 931.0        | 180.7                | 0.3070E 06                      | 1.722                            | 1039.                                     | 6002.                                   |
| 981.0        | 176.6                | 0.3158E 06                      | 1.771                            | 1039.                                     | 5998.                                   |
| 1031.        | 172.9                | 0.3245E 06                      | 1.820                            | 1039.                                     | 5994.                                   |
| 1081.        | 169.4                | 0.3329E 06                      | 1.867                            | 1039.                                     | 5990.                                   |
| 1131.        | 166.3                | 0.3412E 06                      | 1.914                            | 1039.                                     | 5987.                                   |
| 1181.        | 163.4                | 0.3494E 06                      | 1.960                            | 1039.                                     | 5983.                                   |
| 1231.        | 160.7                | 0.3575E 06                      | 2.005                            | 1039.                                     | 5979.                                   |
| 1281.        | 158.2                | 0.3654E 06                      | 2.049                            | 1039.                                     | 5976.                                   |
| 1331.        | 155.9                | 0.3732E 06                      | 2.093                            | 1039.                                     | 5972.                                   |
| 1381.        | 153.7                | 0.3808E 06                      | 2.136                            | 1039.                                     | 5969.                                   |
| 1431.        | 151.6                | 0.3884E 06                      | 2.178                            | 1039.                                     | 5966.                                   |
| 1481.        | 149.7                | 0.3959E 06                      | 2.220                            | 1039.                                     | 5962.                                   |
| 1531.        | 147.9                | 0.4033E 06                      | 2.262                            | 1039.                                     | 5959.                                   |
| 1581.        | 146.1                | 0.4106E 06                      | 2.303                            | 1039.                                     | 5956.                                   |
| 1630.        | 144.5                | 0.4177E 06                      | 2.343                            | 1039.                                     | 5953.                                   |

## APPENDIX D

GASWAT is a two-dimensional reservoir model designed to simulate the flow of both gas and water in porous media. GASWAT is a fully implicit, finite difference model developed specifically for a hydraulically fractured gas well. The model was built to account for reservoir heterogeneity, formation damage, capillary pressure, gas permeability hysteresis, non-Darcy flow effects, and fracture closure. The fracture length, fracture width, and drainage area are all controlled by the grid pattern. The grid patterns used for the three different cases are illustrated in Table D-1.

Table D-2 shows the input data needed for this computer model. The model is equipped with a parameter called QMIN, which is analogous to the minimum or critical gas velocity. QMIN is defined as the critical or minimum gas flow rate required to lift the water out of the wellbore. Once the gas flow rate drops below QMIN, no more water will be produced. This leads to water piling up around and in the fracture. Also included in the input data are the control keys for non-Darcy flow effects, fracture closure, and gas permeability hysteresis. If the capillary pressure multiplier is set equal to zero, the model will neglect the effects of capillary pressure. The output from GASWAT is divided into two sections: the actual time steps and a summary table. Table D-3 shows the actual time step, while Table D-4 illustrates the summary table, which is just a composite of every time step.

TABLE D-1  
 GRID PATTERNS USED FOR COMPUTER MODEL GASWAT

DRAINAGE AREA = 640 ACRES

| <u>Fracture<br/>Length<br/>(ft)</u> | <u>Length of Cells in x-direction (ft)</u>                                |
|-------------------------------------|---|
| 750                                 | 5, 15, 45, 135, 350, 135, 45, 15, 5, 5, 15, 45, 135,<br>563, 563, 564     |
| 1300                                | 5, 15, 45, 135, 450, 450, 135, 45, 15, 5, 5, 15, 45,<br>135, 570, 570     |
|                                     | <u>Length of Cells in y-direction (ft)</u>                                |
|                                     | 0.003, 0.001, 0.005, 1.995, 4.5, 13.5, 40.5, 121.5,<br>400, 686, 686, 686 |

TABLE D-2  
INPUT DATA FOR COMPUTER MODEL GASWAT

## RESERVOIR DATA

|                              |             |        |
|------------------------------|-------------|--------|
| ORIGINAL PRESSURE            | - PSI       | 6134.  |
| ORIGINAL WATER SATURATION    | - FRACTION  | 0.205  |
| IRREDUCIBLE WATER SATURATION | - FRACTION  | 0.127  |
| FORMATION PERMEABILITY       | - MD        | 0.0012 |
| TOTAL POROSITY               | - FRACTION  | 0.057  |
| NET PAY                      | - FEET      | 196.0  |
| FRACTURE PERMEABILITY        | - MD        | 3.5E05 |
| FRACTURE POROSITY            | - FRACTION  | 0.200  |
| FRACTURE LENGTH              | - FEET      | 900.0  |
| CRITICAL GAS FLOW RATE       | - MSCF/D    | -500.0 |
| BOTTOMHOLE TREATING PRESSURE | - PSI       | 8100.  |
| BOTTOMHOLE TEMPERATURE       | - DEGREES F | 285.0  |
| GAS GRAVITY                  | (AIR=1)     | 0.600  |
| DRAINAGE AREA                | - ACRES     | 640    |

## WELL CONTROL DATA

|  |              |       |
|--|--------------|-------|
| NON-DARCY FLOW EFFECTS   |              | YES   |
| FRACTURE CLOSURE AND PERMEABILITY REDUCTION EFFECTS                    |              | YES   |
| GAS PERMEABILITY HYSTERESIS  |              | NO    |
| CAPILLARY PRESSURE MULTIPLIER  |              | 1.0   |
| CONSTANT 'A' IN COOKE'S EQN. FOR                                       |              | 1.54  |
| CONSTANT 'B' IN COOKE'S EQN. FOR                                       |              | 2.65  |
| CONVERGENCE CRITERIA FOR PRESSURE                                      | - PSI        | 1.0   |
| CONVERGENCE CRITERIA FOR SATURATION                                    | - FRACTION   | 0.005 |
| MAXIMUM GAS PRODUCED PER STEP  | - 1/4 OF GIP | 5.0   |
| MAXIMUM PRESSURE DROP PER STEP IN ANY CELL                             | - PSI        | 2000. |
| MAXIMUM SATURATION CHANGE ALLOWED IN<br>RESERVOIR GRID BLOCKS PER STEP | - FRACTION   | 0.25  |
| MAXIMUM SATURATION CHANGE ALLOWED IN<br>FRACTURE GRID BLOCKS PER STEP  | - FRACTION   | 0.50  |

## CONSTANT PRESSURE SCHEDULE

| INTERVAL | LENGTH OF<br>INTERVAL<br>(DAYS) | TIME STEP<br>SIZE<br>(DAYS) | BOTTOMHOLE<br>PRESSURE<br>(PSIA) |
|----------|---------------------------------|-----------------------------|----------------------------------|
| 1        | 14.                             | 25.00                       | 5000.0                           |
| 2        | 7286.                           | 50.00                       | 1039.0                           |



TABLE D-4  
SUMMARY TABLE FROM COMPUTER MODEL GASWAT

| TIME<br>DAYS | GAS<br>FLOW<br>RATE<br>MSFD | WATER<br>FLOW<br>RATE<br>STBD | GAS<br>CUMULATIVE<br>PRODUCTION<br>MSF | WATER<br>CUMULATIVE<br>PRODUCTION<br>STB | AVERAGE<br>RESERVOIR<br>PRESSURE<br>PSI |
|--------------|-----------------------------|-------------------------------|--|--|---|
| 0.1          | -827.9                      | -472.9                        | 0.5948E+02                             | 41.5                                     | 6133.8                                  |
| 0.2          | -701.6                      | -330.5                        | 0.1600E+03                             | 88.9                                     | 6133.7                                  |
| 0.6          | -604.2                      | -212.1                        | 0.4197E+03                             | 180.0                                    | 6133.4                                  |
| 1.9          | -601.2                      | -134.9                        | 0.1195E+04                             | 354.0                                    | 6132.9                                  |
| 5.8          | -490.3                      | -66.5                         | 0.3092E+04                             | 611.1                                    | 6131.9                                  |
| 14.1         | -2756.5                     | -464.2                        | 0.6622E+04                             | 934.9                                    | 6130.0                                  |
| 15.1         | -2070.7                     | -229.4                        | 0.8708E+04                             | 1183.5                                   | 6128.7                                  |
| 17.3         | -1793.0                     | -137.6                        | 0.1263E+05                             | 1484.5                                   | 6126.7                                  |
| 23.8         | -1436.6                     | -69.5                         | 0.2205E+05                             | 1940.4                                   | 6122.2                                  |
| 43.5         | -1045.5                     | -29.6                         | 0.4263E+05                             | 2523.8                                   | 6113.1                                  |
| 93.5         | -705.7                      | -11.9                         | 0.7792E+05                             | 3118.3                                   | 6097.8                                  |
| 143.5        | -540.6                      | -6.7                          | 0.1049E+06                             | 3451.8                                   | 6086.2                                  |
| 193.5        | -466.4                      | -3.8                          | 0.1283E+06                             | 3642.1                                   | 6076.5                                  |
| 243.5        | -414.7                      | -2.2                          | 0.1490E+06                             | 3752.7                                   | 6067.9                                  |
| 293.5        | -371.4                      | -1.2                          | 0.1676E+06                             | 3814.7                                   | 6060.2                                  |
| 343.5        | -343.8                      | -0.6                          | 0.1848E+06                             | 3843.8                                   | 6053.1                                  |
| 393.5        | -324.1                      | -0.1                          | 0.2010E+06                             | 3849.3                                   | 6046.4                                  |
| 443.5        | -308.7                      | -0.1                          | 0.2164E+06                             | 3854.1                                   | 6040.1                                  |
| 493.5        | -296.0                      | -0.2                          | 0.2312E+06                             | 3862.3                                   | 6034.0                                  |
| 543.5        | -276.4                      | -0.1                          | 0.2450E+06                             | 3869.8                                   | 6028.0                                  |
| 593.5        | -265.4                      | -0.1                          | 0.2583E+06                             | 3876.8                                   | 6022.4                                  |
| 643.5        | -255.0                      | -0.1                          | 0.2710E+06                             | 3883.4                                   | 6016.9                                  |
| 693.5        | -242.6                      | -0.1                          | 0.2832E+06                             | 3889.6                                   | 6011.7                                  |
| 693.7        | -247.2                      | 0.0                           | 0.2832E+06                             | 3889.6                                   | 6011.6                                  |
| 694.0        | -243.1                      | 0.0                           | 0.2833E+06                             | 3889.6                                   | 6011.6                                  |
| 694.7        | -202.0                      | 0.0                           | 0.2834E+06                             | 3889.6                                   | 6011.5                                  |
| 702.2        | -87.8                       | 0.0                           | 0.2839E+06                             | 3889.6                                   | 6011.1                                  |
| 719.0        | -4.3                        | 0.0                           | 0.2840E+06                             | 3889.6                                   | 6010.7                                  |
| 769.0        | -39.5                       | 0.0                           | 0.2860E+06                             | 3889.6                                   | 6009.1                                  |
| 819.0        | -59.1                       | 0.0                           | 0.2889E+06                             | 3889.6                                   | 6007.2                                  |
| 869.0        | -92.0                       | 0.0                           | 0.2935E+06                             | 3889.6                                   | 6005.2                                  |
| 919.0        | -104.4                      | 0.0                           | 0.2987E+06                             | 3889.6                                   | 6003.0                                  |
| 969.0        | -93.6                       | 0.0                           | 0.3034E+06                             | 3889.6                                   | 6000.9                                  |
| 1019.0       | -86.3                       | 0.0                           | 0.3077E+06                             | 3889.6                                   | 5998.9                                  |
| 1069.0       | -83.5                       | 0.0                           | 0.3119E+06                             | 3889.6                                   | 5996.9                                  |
| 1119.0       | -81.9                       | 0.0                           | 0.3160E+06                             | 3889.6                                   | 5994.9                                  |
| 1169.0       | -123.0                      | 0.0                           | 0.3221E+06                             | 3889.6                                   | 5993.0                                  |
| 1219.0       | -103.3                      | 0.0                           | 0.3273E+06                             | 3889.6                                   | 5991.1                                  |
| 1269.0       | -91.7                       | 0.0                           | 0.3319E+06                             | 3889.6                                   | 5989.1                                  |
| 1319.0       | -121.5                      | 0.0                           | 0.3380E+06                             | 3889.6                                   | 5987.2                                  |
| 1369.0       | -119.0                      | 0.0                           | 0.3439E+06                             | 3889.6                                   | 5985.3                                  |
| 1419.0       | -96.0                       | 0.0                           | 0.3487E+06                             | 3889.6                                   | 5983.3                                  |
| 1469.0       | -120.8                      | 0.0                           | 0.3548E+06                             | 3889.6                                   | 5981.4                                  |
| 1519.0       | -101.4                      | 0.0                           | 0.3598E+06                             | 3889.6                                   | 5979.4                                  |

## VITA

**Name:** Charles Edward Pietsch

**Born:** March 28, 1963  
Altus, Oklahoma

**Parents:** Edward and Betty Pietsch

**Permanent Address:** 12009 Tall Forest  
Cypress, Texas 77429

**University:** Texas A & M University  
College Station, Texas  
Bachelor of Science Degree in  
Petroleum Engineering (May 1985)

Texas A & M University  
College Station, Texas  
Master of Science Degree in  
Petroleum Engineering (August 1986)